Portland Cement Association

Research & Development Information

PCA R&D Serial No. 0887

Heat Transfer Characteristics of a Structural Lightweight Concrete Wall

by M. G. VanGeem and A. E. Fiorato

5420 Old Orchard Road
Skokie, Illinois 60077-1083
847.966.6200 Fax 847.966.9481

www.cement.org

PCA R&D Serial No. 0887

HEAT TRANSFER CHARACTERISTICS OF A STRUCTURAL LIGHTWEIGHT CONCRETE WALL

Report to

OAK RIDGE NATIONAL LABORATORIES
Oak Ridge, Tennessee 37830
Operated by
Union Carbide Corporation

Prepared for the
Office of Buildings Energy
Research and Development
U.S. Department of Energy
Under Subcontract No.
ORNL/SUB-42539/2

Final Report

by

M. G. Van Geem and A. E. Fiorato

Submitted by

CONSTRUCTION TECHNOLOGY LABORATORIES
A Division of the Portland Cement Association
5420 Old Orchard Road
Skokie, Illinois 60077

June 1983

TABLE OF CONTENTS

TABLE OF CONTENTS (continued)

LIST OF TABLES

LIST OF FIGURES

LIST OF FIGURES (continued)

HEAT TRANSFER CHARACTERISTICS OF A STRUCTURAL LIGHTWEIGHT CONCRETE WALL

by

M. G. Van Geem and A. E. Fiorato

ABSTRACT

Tests were conducted to evaluate thermal performance of three concrete walls. A normal-weight concrete wall, a structural lightweight concrete wall, and a low density concrete wall were tested in the calibrated hot box facility of Construction Technology Laboratories, a division of the Portland Cement Association. This report covers experimental results for the structural lightweight concrete wall. Test results for the normal-weight concrete wall and low density concrete wall are covered in separate reports.

The wall was subjected to steady-state, transient, and periodically varying temperature conditions in a calibrated hot box. Steady-state tests were used to define heat transmission coefficients. Data obtained during transient and periodic temperature variations were used to define dynamic thermal response of the wall. Thus, effects of heat storage capacity could be evaluated.

Conductivities derived from calibrated hot box tests were compared with results from hot wire tests. Hot wire tests were also used to evaluate the influence of moisture on thermal conductivity. Data obtained from dynamic tests were compared with steady-state calculations.

Data obtained in this investigation are applicable to concrete wall assemblies commonly used in multi-family residential, commercial, and industrial structures. Results provide a data base for evaluation of building envelope performance in such structures, and are also applicable for defining thermal characteristics of concrete walls in passive solar systems.

HEAT TRANSFER CHARACTERISTICS OF A STRUCTURAL LIGHTWEIGHT CONCRETE WALL

by

M. G. Van Geem and A. E. Fiorato*

INTRODUCTION

Tests were conducted to evaluate thermal performance of solid concrete walls under steady-state and dynamic temperature conditions. Steady-state tests were used to obtain average heat transmission coefficients including thermal conductivity, total thermal resistance (R_T), and thermal transmittance (U). Dynamic tests provided a measure of thermal response under selected temperature ranges. A simulated sol-air dynamic cycle was selected to permit comparison of results with those obtained in previous investigations.(1-3)**

Objectives of the experimental investigation were to evaluate and compare thermal performance of three concrete walls. Wall C1 was constructed of normal-weight structural concrete, Wall C2 was constructed of structural lightweight concrete, and Wall C3 was constructed of low density concrete. This report covers experimental results of Wall C2. Walls C1 and C3 are covered in separate reports.(4,5)

*Respectively, Research Engineer, Construction Methods Department, and Director, Concrete Materials Research Department, Construction Technology Laboratories, a Division of the Portland Cement Association, 5420 Old Orchard Road, Skokie, Illinois 60077.

**Superscript numbers in parentheses refer to references listed at the end of this report.

Also included in this report are data on thermal properties of control specimens cast from the same concrete used to cast Wall C2. Results are compared with test data for similar types of concrete.

Walls were tested in the calibrated hot box facility of Portland Cement Association's Construction Technology Laboratories (CTL).

TEST SPECIMEN

Wall C2 was a structural lightweight concrete wall with an average thickness of 8.28 in. (210 mm). The wall was cast horizontally and has overall nominal dimensions of 103x103 in. (2.62x2.62 m). All wall construction, including concrete mixing and casting, was performed at CTL. Expanded shale aggregate with a nominal maximum size of 3/4 in. (19 mm) was used in the concrete.

The mix design for the structural lightweight concrete wall is given in Table 1. The water-cement ratio was 0.66. Average measured slump of the fresh concrete was 2.8 in. (71 mm). Average measured air content was 6.3%. Average fresh unit weight of the concrete was 103.1 pcf (1652 kg/m^3).

Reinforcement consisted of a single layer of No. 5 bars in each direction detailed as shown in Fig. 1. Reinforcing bars, spaced 12 in. (305 mm) center-to-center, were supported at a height of 4 in. (102 mm) off the formwork base by concrete chairs. Chair supports, shown in Fig. 2, were constructed using the same concrete mix used for construction of Wall C2.

TABLE 1 - WALL C2 MIX DESIGN

Material	Quantities per cu yd of concrete
Type I Cement	519 lb (236 kg)
Water	340 lb (155 kg)
Coarse Expanded Shale+, No. 4 - 3/4" SSD* (7.04% MC**)	780 lb (355 kg)
Fine Expanded Shale++, SSD (5% MC**)	1150 lb (523 kg)
Vinsol Resin - 2.2% Solution (Air-Entraining Admixture)	1.75 ml/lb cement

*Saturated surface dry; neither absorbing water from nor contributing water to the concrete mix(6)

**Moisture content, by ovendry weight

+Ovendry unit weight of coarse expanded shale was 49 pcf (780 kg/m^3).

++Ovendry unit weight of fine expanded shale was 65 pcf (1030 kg/m^3).

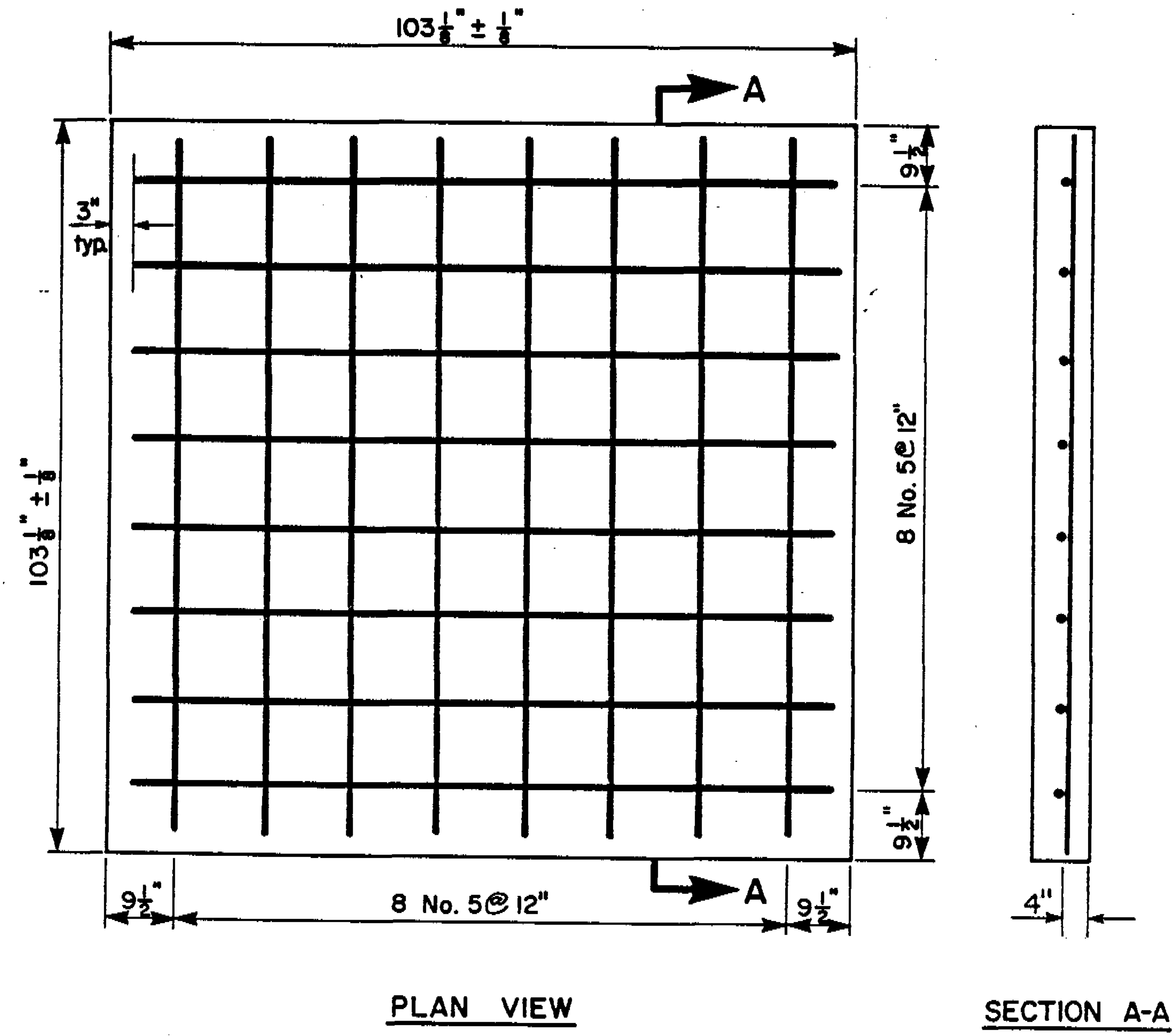

Fig. 1 Reinforcement Details for Structural Lightweight Concrete Wall C2

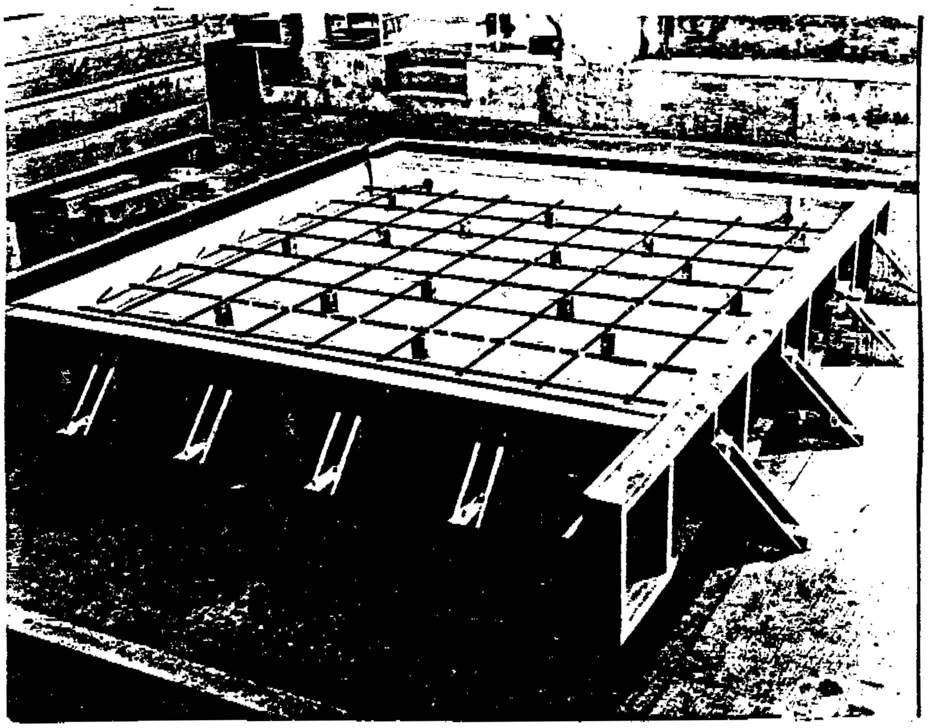

Fig. 2 Formwork and Reinforcement for Wall C2

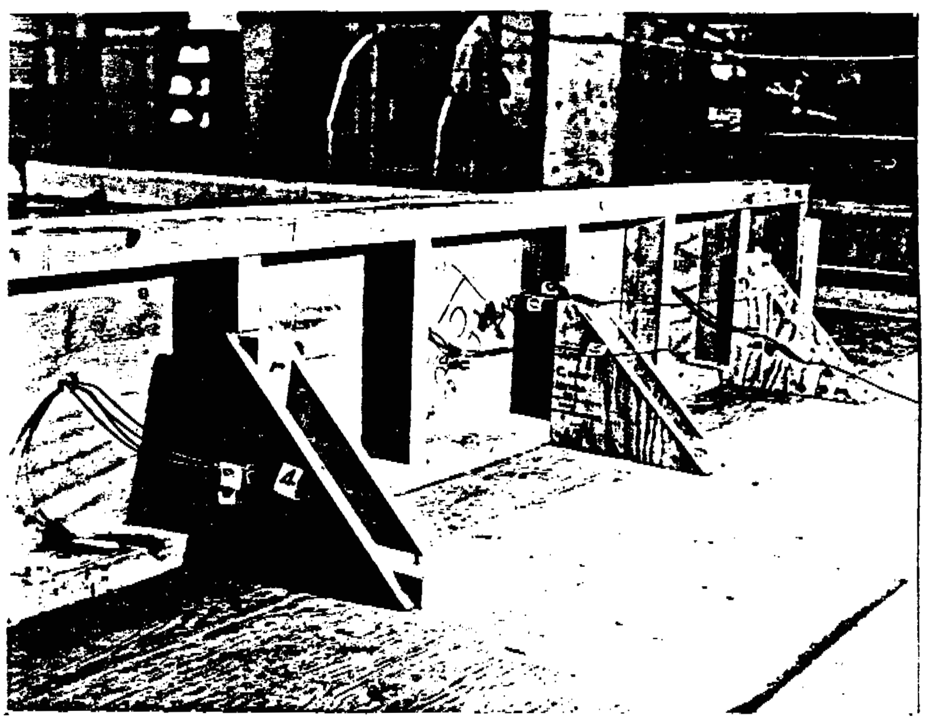

Fig. 3 Thermocouple Wire Leads

Concrete rather than steel or plastic chairs were used since precise measurement of wall thermal properties required the elimination of possible thermal bridges.

Threaded coil inserts were cast into the wall at midthickness to aid in transporting the wall after concrete had attained sufficient strength. Inserts are shown projecting through the side formwork at the top of Fig. 2.

Thermocouple wires were cast into the concrete wall at the same level as the reinforcing bars. Thermocouple leads penetrated the formwork edge, as shown in Fig. 3. A more detailed discussion of thermocouple placement and instrumentation is included in the subsection entitled, "Instrumentation" of the "Calibrated Hot Box Test Facility," section.

Ten 6-cu ft batches of concrete were prepared for Wall C2. Concrete was mixed using a 6-cu ft concrete mixer and was transported in a concrete bucket by forklift to the casting site. The concrete bucket was lifted above formwork by an overhead crane and concrete was placed in the formwork. Concrete was placed horizontally in a full thickness from one side of the wall to the opposite side. The concrete was consolidated using an internal vibrator. After the formwork was filled and concrete was consolidated, the top surface was screeded, and then finished. Plastic sheets were used to cover the surface of the wall for curing.

Wall C2 was allowed to cure in formwork for seven days. After removing formwork, the wall was allowed to air cure in the laboratory at an air temperature of 73±5°F (23±3°C) and 45±15% RH for five months prior to testing.

Faces of Wall C2 were coated with a cementitious waterproofing material that seals minor surface imperfections. A textured, noncementitious white paint was used as a finish coat. These coatings provided a uniform surface for both wall faces. Wall edges were left uncoated. Figure 4 shows Wall C2 prior to testing.

At the time Wall C2 was cast, control specimens were cast for measurement of selected physical and thermal properties. Control specimens were taken, as detailed in Table 2, from each of the ten batches required to cast Wall C2. Each specimen was cast in individual molds and placed on a vibrating table to consolidate the concrete.

PHYSICAL PROPERTIES OF CONCRETE

Unit weight, moisture content, compressive strength, and tensile splitting strength of 6x12-in. (152x305-mm) cylinders were determined. Unit weight of Wall C2 was also determined by measuring total weight of the wall. Physical properties are summarized in Table 3.

Unit Weight

Weights of Wall C2 and seven 6x12-in. (152x305-mm) cylinders were determined periodically while the specimens were air drying. The volume of Wall C2 was determined from average measured dimensions of each side and average wall thickness. Volume of each cylinder was calculated from cylinder weights in air and

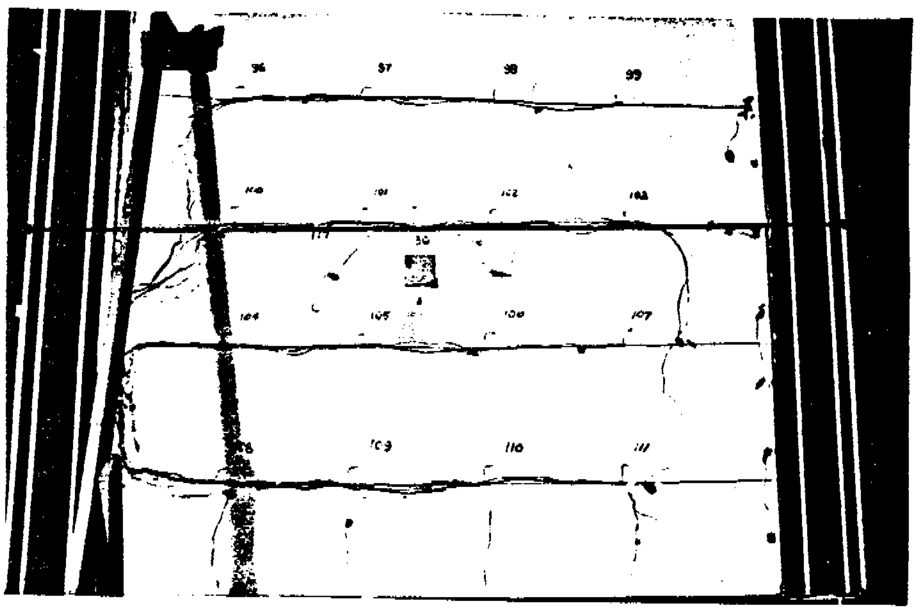

Fig. 4 Wall C2 Prior to Testing

TABLE 2 - SPECIMENS FOR MEASUREMENT OF SELECTED THERMAL AND PHYSICAL PROPERTIES OF WALL C2

Concrete Batch No.	6x12-in. (152x305-mm) Cylinders			4x4x8-in. (102x102x203-mm) Prisms for Thermal Conductivity by Hot Wire Method	16x16x2-in. (406x406x51-mm) Prisms for Thermal Conductivity by Hot Plate Method	3x6-in. (76x152-mm) Cylinders for Specific Heat Tests
	Compressive Strength Tests	Splitting Tensile Strength Tests	Thermal Diffusivity Tests			
1	1	1	1	1	-	1
2	1	1	1	1	-	1
3	1	-	1	-	-	1
4	1	1	-	1	1	1
5	1	-	1	-	-	1
6	1	1	-	1	1	1
7	1	-	1	-	-	1
8	1	1	-	1	1	1
9	1	-	1	-	-	1
10	1	1	-	1	1	1
Total	10	6	6	6	4	10

TABLE 3 - PHYSICAL PROPERTIES OF WALL C2

Property	Measured Value
Unit Weight of Wall, pcf (kg/m^3)	102 (1630)
Estimated Moisture Content of Wall, % ovendry weight	8.5
Average Thickness, in. (mm)	8.28 (210)
Area, ft^2 (m^2)	73.67 (6.844)
Concrete Compressive Strength, psi (MPa)	
moist cured*	3820 (26.3)
air cured**	5350 (36.9)
Concrete Splitting Tensile Strength, psi (MPa)	
moist cured*	390 (2.70)
air cured**	435 (3.00)

*Cured in molds for first 24 hours, moist cured for 27 days.
**Cured in molds for first 7 days, air cured for 184 days.

immersed in water. Unit weights then were calculated from measured weights and volumes.

Unit weights for Wall C2 and the 6x12-in. (152x305-mm) cylinders are summarized in Table 4 and Fig. 5. Unit weights decreased with time for the first two months and then remained fairly constant. The reduction in unit weight is due to evaporation of free water from concrete.

Equilibrium water contents are generally attained when the concrete is in equilibrium with air on all sides, and undergoes no further change in weight. Concrete is generally considered normally dry when the free water in the concrete has attained an equilibirum after an extended period of drying at 35 to 50% relative humidity.(7) For this report it is assumed that the concrete of Wall C2 was normally dry after five months of air curing. Using this assumption, the unit weight of Wall C2 in the normally dry state is taken to be 102 pcf (1630 kg/m^3). Average unit weight of seven cylinders in the normally dry state is 100 pcf (1600 kg/m^3).

Moisture Content

Average moisture content of Wall C2 at the time of calibrated hot box tests was determined from air dry unit weight of the wall and average ovendry unit weight of four control specimens. Air dry unit weight of Wall C2 at the time of calibrated hot box tests was 102 pcf (1630 kg/m^3). Curing conditions and ovendry unit weights of four 4x4x8-in. (102x102x203-mm) prisms prepared for hot wire thermal conductivity tests are shown in Table 5.

TABLE 4 - UNIT WEIGHT OF WALL AND CONTROL SPECIMENS

Age days	Wall C2, pcf (kg/m^3)	Average for Seven Cylinders, pcf (kg/m^3)
0	103.1 (1652)	103.1 (1652)
7	105.9 (1697)	105.1 (1684)
14	104.3 (1671)	103.0 (1650)
28	103.5 (1658)	102.0 (1634)
64	102.4 (1640)	101.6 (1628)
84	102.9 (1648)	101.2 (1621)
112	103.1 (1652)	100.8 (1615)
148	102.8* (1647)	100.1 (1604)
191	101.6** (1628)	99.9 (1600)

*Unit weight of Wall C2 at 145 days
**Unit weight of Wall C2 at 211 days

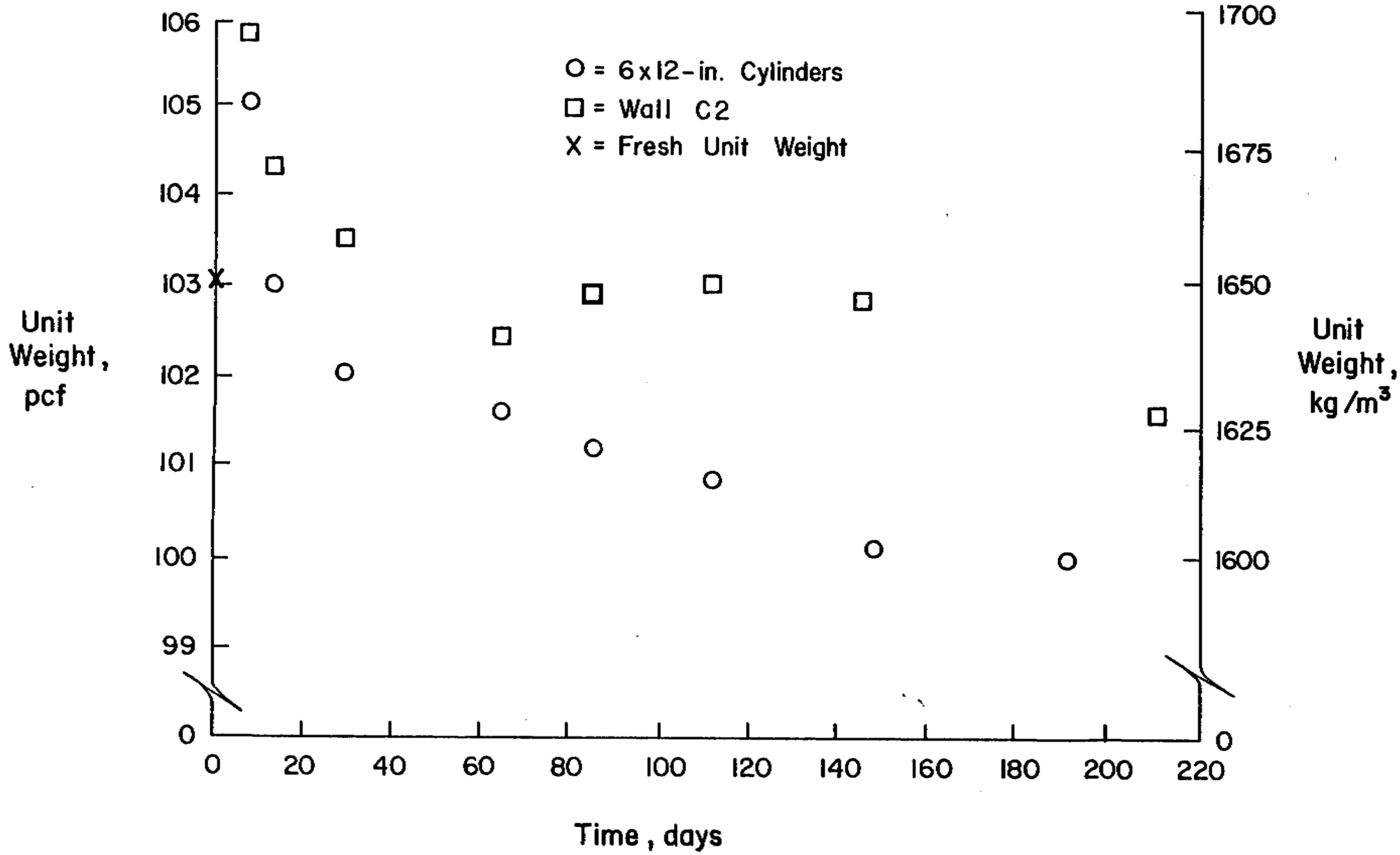

Fig. 5 Unit Weight of Wall C2 and Control Cylinders as a Function of Time

TABLE 5 - OVENDRY UNIT WEIGHTS OF CONTROL SPECIMENS FOR WALL C2

Curing Conditions	Age at Time of Weight Measurement, days	Specimen No.	Unit Weight, pcf (kg/m^3)
7 days in Mold; 168 days Air Dry 73°F (23°C) 45% RH; Ovendry	175	2H	93.6 (1499)
		6H	93.3 (1495)
		10H	96.4 (1545)
24 hours in Mold; 119 days Moist Cure 73°F (23°C) 100% RH; 63 days Air Dry 73°F (23°C) 45% RH; Ovendry	183	4G	92.9 (1489)
-----	---	Average	94.1 (1507)

Assuming the ovendry unit weight of Wall C2 is equal to the average ovendry unit weight of the control specimens, Wall C2 has an estimated ovendry unit weight of 94 pcf (1510 kg/m^3). Therefore, average moisture content relative to ovendry weight of Wall C2 is estimated to be 8.5% at the time of test.

Compressive Strength

Compressive strength of 6x12-in. (152x305-mm) concrete cylinders was determined in accordance with ASTM Designation: C39 "Standard Test Method for Compressive Strength of Cylindrical Concrete Specimens."(8) Two sets of data were obtained as follows:

1. Twenty-eight-day compressive strengths of five cylinders cured for 24 hours in molds, and then moist cured at 73±3°F (23±1.7°C) and 100% RH the remaining 27 days
2. One hundred ninety-one-day compressive strengths of four cylinders cured in molds for seven days, and then air cured at 73±5°F (23±3°C) and 45±15% RH until Wall C2 was midway through thermal tests

Table 6 summarizes compressive strength results for moist cured 6x12-in. (152x305-mm) cylinders and air cured 6x12-in. (152x305-mm) cylinders.

Splitting Tensile Strength

Splitting tensile strength of 6x12-in. (152x305-mm) concrete cylinders was determined in accordance with ASTM Designation: C496 "Standard Test Method for Splitting Tensile Strength of

TABLE 6 - COMPRESSIVE STRENGTH OF CONTROL CYLINDERS FOR WALL C2

Specimen No.	Moist Cured*		Specimen No.	Air Cured**	
	Unit Weight, pcf (kg/m^3)	Compressive Strength, psi (MPa)		Unit Weight, pcf (kg/m^3)	Compressive Strength, psi (MPa)
1A	106.2 (1701)	3660 (25.2)	4B	100.1 (1603)	5290 (36.5)
3A	107.7 (1725)	3810 (26.3)	6B	97.9 (1568)	4770 (32.9)
5A	107.0 (1714)	4400 (30.3)	8B	101.1 (1619)	5480 (37.8)
7A	106.7 (1709)	3620 (25.0)	10B	101.4 (1624)	5850 (40.3)
9A	104.9 (1680)	3610 (24.9)			
Average	106.5 (1706)	3820 (26.3)	Average	100.1 (1603)	5350 (36.9)

*Cured in molds for first 24 hours, moist cured for 27 days
**Cured in molds for first 7 days, air cured for 184 days

Cylindrical Concrete Specimens."(8) Two sets of data were obtained as follows:

1. Twenty-eight-day splitting tensile strengths of three cylinders cured for 24 hours in molds, and then moist cured at 73±3°F (23±1.7°C) and 100% RH the remaining 27 days
2. Splitting tensile strengths of cylinders cured in molds for seven days, and then cured at 73±5°F (23±3°C) and 45±15% RH until Wall C2 was midway through thermal tests

Table 7 summarizes splitting tensile strength results for moist cured and air cured 6x12-in. (152x305-mm) cylinders.

CALIBRATED HOT BOX TEST FACILITY

Tests were conducted in the calibrated hot box facility shown in Fig. 6. This facility was developed to permit realistic evaluation of thermal performance of large wall assemblies under steady-state or dynamic temperature conditions. Tests were performed in accordance with ASTM Designation: C976, "Standard Test Method for Thermal Performance of Building Assemblies by Means of a Calibrated Hot Box."(8)

Description

The following is a brief description of the calibrated hot box. Details are available in Reference 9. The facility consists of two highly insulated chambers as shown in Fig. 7. Walls, ceiling, and floors of each chamber were insulated with foamed urethane sheets to obtain a final thickness of 12 in.

TABLE 7 - SPLITTING TENSILE STRENGTH OF CONTROL CYLINDERS FOR WALL C2

Specimen No.	Moist Cured*		Specimen No.	Air Cured**	
	Unit Weight, pcf (kg/m^3)	Splitting Tensile Strength, psi (MPa)		Unit Weight, pcf (kg/m^3)	Splitting Tensile Strength, psi (MPa)
1C	106.1 (1700)	423 (2.92)	2D	100.5 (1610)	434 (2.99)
4C	106.4 (1704)	357 (2.46)	6D	97.7 (1565)	430 (2.96)
8C	107.2 (1717)	392 (2.70)	10D	100.9 (1616)	438 (3.02)
Average	106.6 (1708)	391 (2.70)	Average	99.7 (1597)	434 (2.99)

*Cured in molds for first 24 hours, moist cured for 27 days
**Cured in molds for first 7 days, air cured for 184 days

Fig. 6   Calibrated Hot Box Test Facility

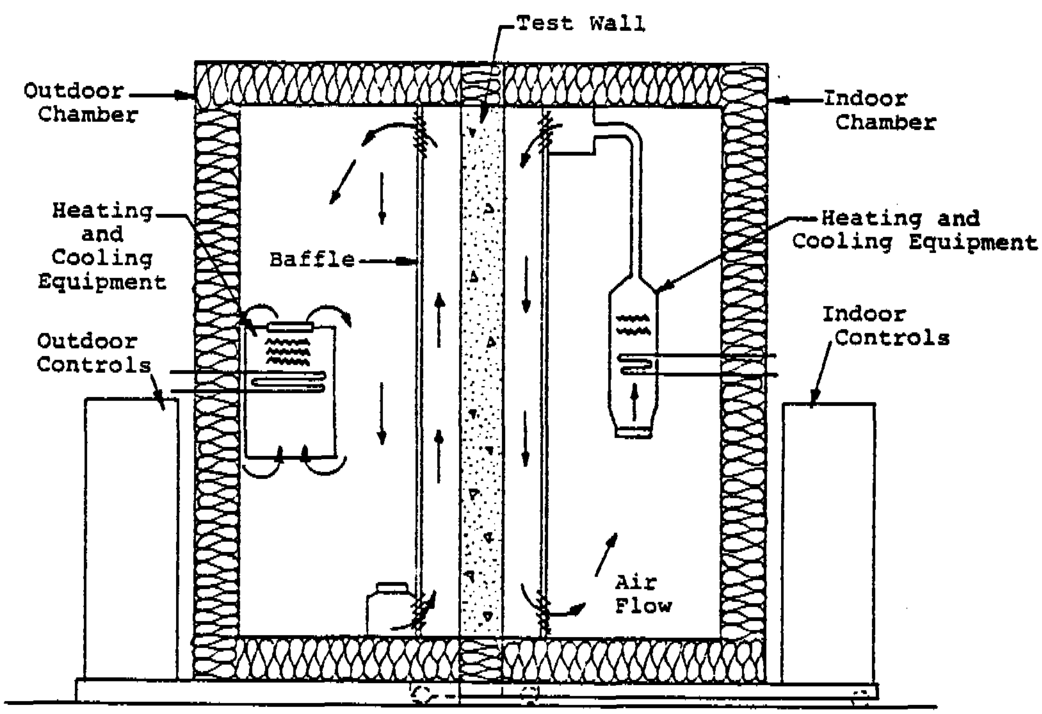

Fig. 7   Schematic of Calibrated Hot Box

(305 mm). During tests, the chambers are clamped tightly against an insulating frame that surrounds the test wall. Air in each chamber is conditioned by heating and cooling equipment to obtain desired temperatures on each side of the test wall.

The outdoor chamber can be held at a constant temperature or cycled between -15 and 130°F (-26 and 54°C). Temperature cycles can be programmed to obtain the desired time-temperature relationship. The indoor chamber, which simulates an indoor environment, can be maintained at a constant room temperature between 65 and 80°F (18 and 27°C).

The facility was designed to accommodate walls with thermal resistance values ranging from 1.5 to 20 $hr \cdot ft^2 \cdot °F/Btu$ (0.26 to 3.52$°K \cdot m^2/W$).

Instrumentation

Instrumentation was designed to monitor temperatures inside and outside of the chambers, air and surface temperatures on both sides of the test wall, interior temperatures within the test wall, laboratory air temperature, and heating energy input to the indoor chamber. Supplementary measurements monitor indoor cooling system performance as well as heat flux at selected locations on the specimen and chamber surfaces. Basically, the instrumentation provides a means of monitoring the energy required to maintain constant temperature in the indoor chamber while temperatures in the outdoor chamber are varied. This energy, when corrected for thermal losses, provides a measure of heat flow through the test wall.

Thermocouples corresponding to ASTM Designation: E230, "Standard Temperature-Electromotive Force (EMF) Tables for Thermocouples,"[8] Type T, were used to measure temperatures. There were 16 in the air space of each chamber, 16 on each face of the test wall, and 16 at approximate midthickness of the test wall. Thermocouples were uniformly distributed on a 20-in. (508 mm) square grid over the wall area. Supplementary thermocouples were used to measure surface temperatures at selected locations.

Surface thermocouples were securely attached to the wall over a length of approximately 3 in. (76 mm). Tape that covered the sensors was painted the same color as the test wall surface. Thermocouples in air were located approximately 3 in. (76 mm) from the face of the test wall.

Internal thermocouples were cast 4 in. (102 mm) from the formwork base. To secure their location, thermocouples were taped to reinforcement, as shown in Fig. 8, or suspended by wire between reinforcement, as shown in Fig. 9. Note in Fig. 9 that the thermocouple junction was not placed in contact with the reinforcement. This was done for all internal thermocouples to avoid any influence on internal heat flow through reinforcement. Thermocouples were wired such that an electrical average of four thermocouple junctions, located along a horizontal line across the grid, was obtained. Thermocouple leads were then routed through side formwork, as shown in Fig. 3.

Inside and outside surface temperatures were measured on each wall of the indoor chamber. These temperatures provided

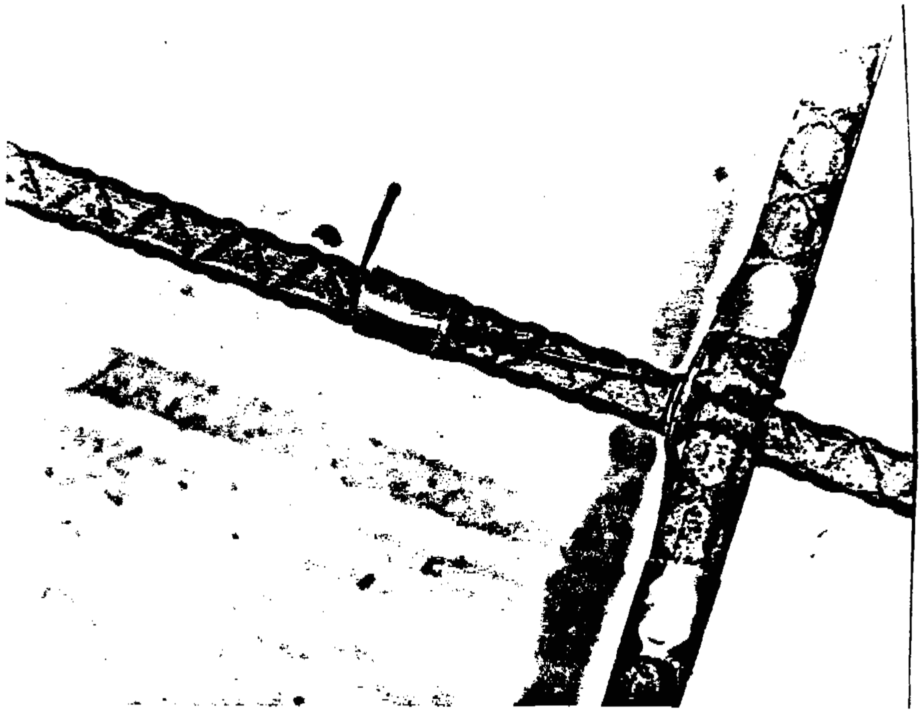

Fig. 8 Mounting of Internal Thermocouple Using Reinforcement as Support

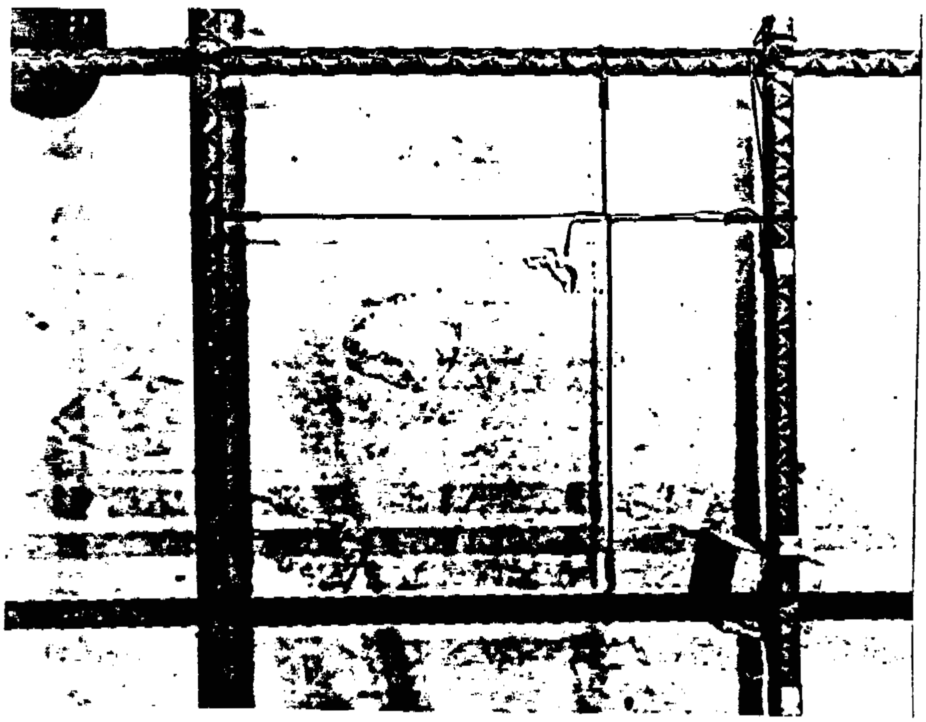

Fig. 9 Mounting of Internal Thermocouple Within Reinforcement Grid

data for evaluating heat transfer between the chamber and the laboratory. Temperature data were supplemented with heat flux transducer measurements.

Heat flux transducers were also mounted on the wall specimen. To do this, 3/8-in. (10-mm) holes were drilled into Wall C2 at selected mounting locations. Wood dowels 3/8-in. (10-mm) in diameter were epoxied in place and sanded flush with the wall surface as shown in Fig. 10. The heat flux transducer surface in contact with the wall surface was coated with a thin layer of high conductivity silicon grease. The heat flux transducer was then mounted on Wall C2 using screws into the wood dowels. The silicon grease provided uniform contact between the heat flux transducer and wall surface. Figure 11 shows a mounted heat flux transducer.

A watt-hour transducer was used to measure cumulative electrical energy input to the indoor chamber. The transducer is calibrated within a specified accuracy of ±0.1% of the measured reading, or approximately 2 watts.

A digital humidity and temperature measurement system was used to measure relative humidity and temperature in air streams on each side of the test specimen. Probes were located in the air streams approximately at the specimen mid-point. The relative humidity sensor is calibrated to within a specified accuracy of ±4%.

Air flow rates in each chamber were measured with air flow meters located approximately at the wall geometric center. Each flow rate meter was mounted perpendicular to the air flow. Data

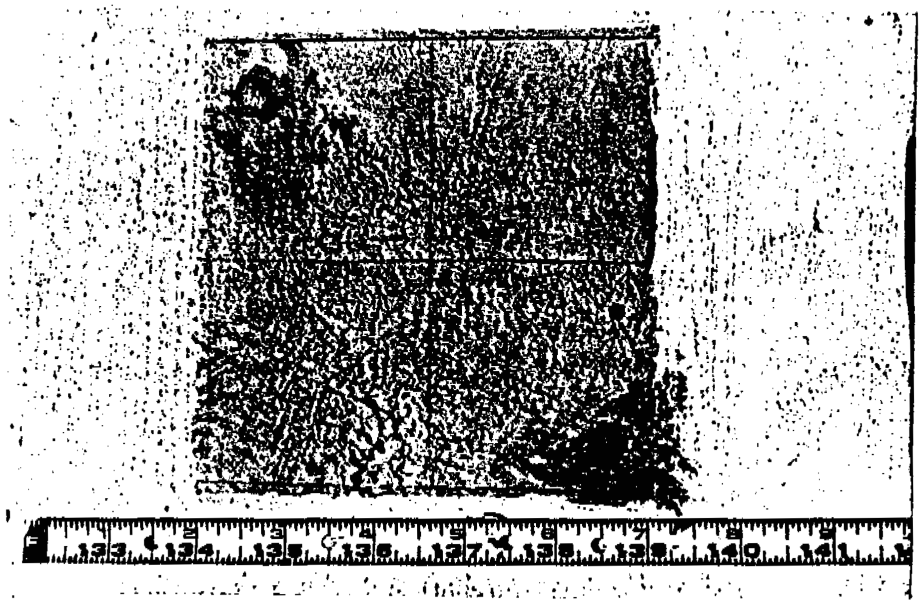

Fig. 10 Wood Dowels Epoxied in Concrete Wall for Heat Flux Transducer Mounting

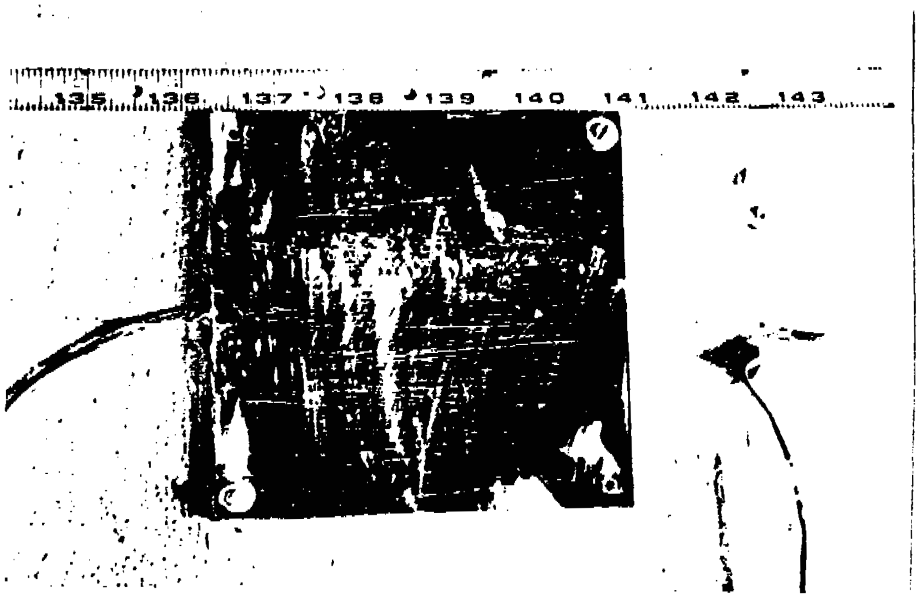

Fig. 11 Heat Flux Transducer Mounted on Wall

for air flow meters were monitored periodically and were not part of the automated data acquisition apparatus.

All measurements, with the exception of air flow rates, were monitored with a programmable digital data acquisition system capable of sampling and recording up to 124 independent channels of data at preselected time intervals. The data acquisition system is interfaced with a microcomputer that is programmed to reduce and store data.

For tests described in this report, thermocouple channels were scanned every two minutes. Average temperature, humidity, and heat flux data were obtained from the 30 readings per hour. The cumulative watt-hour transducer output was scanned every hour.

Calibration Procedure

The following is a brief description of the calibration procedure used for determining heat flow through the test wall. Details are available in Reference 10.

Heat flow through a test wall is determined from measurements of the amount of energy input to the indoor chamber to maintain a constant temperature. The measured energy input must be adjusted for heat losses. Figure 12 shows sources of heat losses and gains by the indoor chamber where:

Q_w = heat transfer through test wall

Q_c = heat removed by indoor chamber cooling

Q_h = heat supplied by indoor electrical resistance heaters

Q_{fan} = heat supplied by indoor circulation fan

Q_ℓ = heat loss/gain from laboratory

Q_f = heat loss/gain from flanking path around specimen

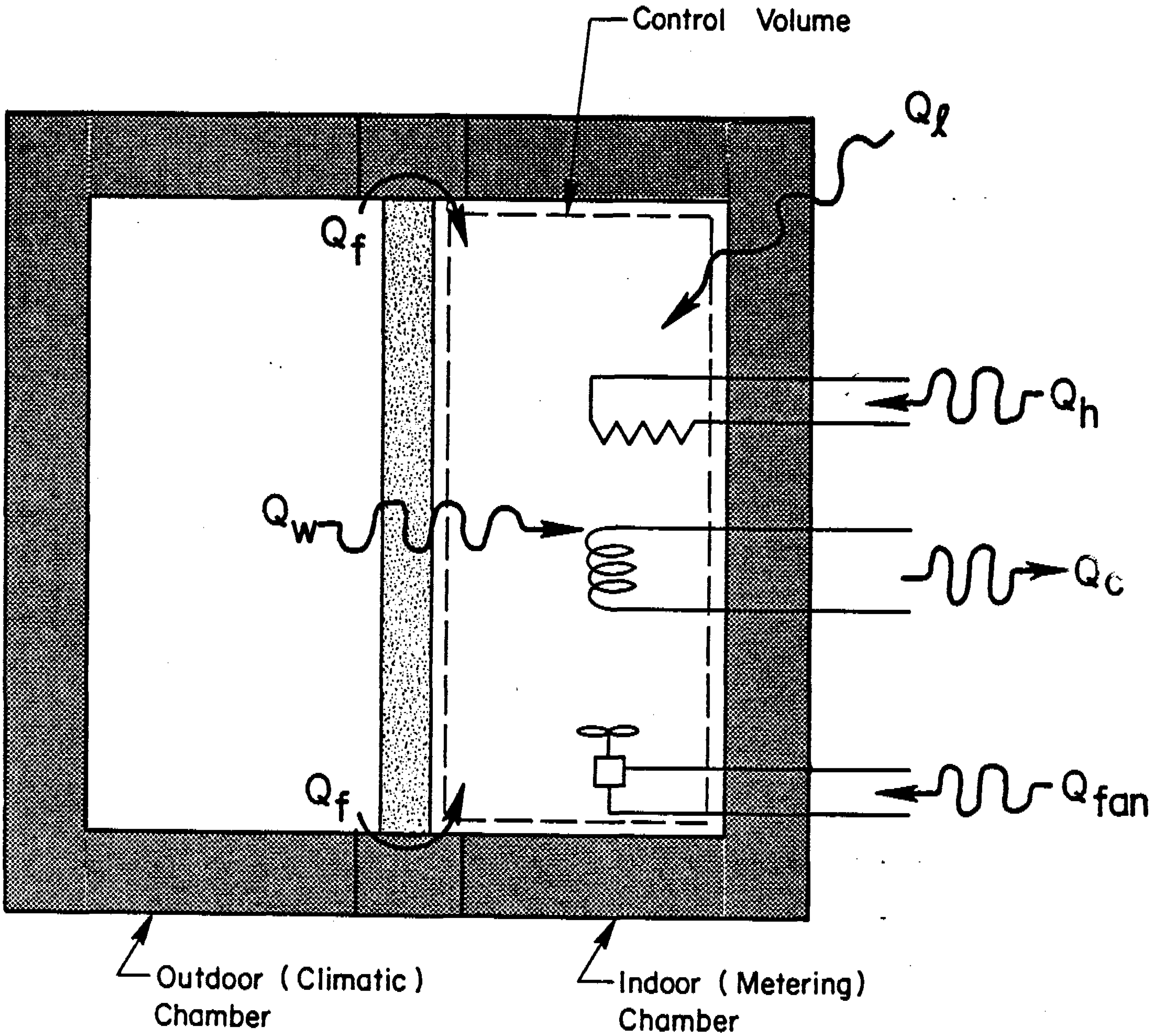

Fig. 12 Indoor (Metering) Chamber Energy Balance

Since net energy into the control volume equals zero, heat transfer through the test wall can be expressed by the following energy balance equation:

$$Q_w = Q_c - Q_h - Q_{fan} - Q_\ell - Q_f \tag{1}$$

The terms Q_h and Q_{fan} are measured by a watt-hour transducer. Heat flux transducers are used to check calculations of Q_ℓ. Steady-state calibrated hot box tests of two "standard" calibration specimens are used to refine calculations of Q_c and to determine Q_f.

The first calibration specimen, S1, has a relatively low thermal resistance of 5.7 hr·ft^2·°F/Btu (1.0 m^2·°K/W). It consists of 1.375-in. (34.9-mm) thick fiberglass and was specially fabricated to insure uniformity.

The second calibration wall, S2, has a relatively high thermal resistance of 17.3 hr·ft^2·°F/Btu (3.0 m^2·°K/W). Material for specimen S2 was selected as part of the ASTM Committee C16 Hot Box Round Robin program. It consists of expanded polystyrene board that is specially produced and cut to insure uniformity. Board faces are coated to provide surfaces suitable for attachment of instrumentation.

Indoor Chamber Cooling

The need for cooling in the indoor chamber results from requirements for dynamic tests. In cases where outdoor temperatures exceed indoor temperatures, cooling capacity is required to maintain indoor temperature control.

Indoor chamber cooling equipment operates continuously and is designed to remove heat at a constant rate. Control of indoor chamber temperature is obtained by varying the amount of input heat required to balance the amount of heat removed by the refrigeration system, the amount of heat that flows through the test specimen, and the amount of heat lost to laboratory space.

Heat removed by indoor chamber cooling is calculated assuming an ideal basic vapor compression refrigeration cycle. Adjustments are made to compensate for inefficiencies in the actual refrigeration cycle.

For the ideal basic vapor compression cycle, the rate of heat transfer between the cooling coils and the indoor chamber is:[11]

$$Q_c' = (h_2 - h_1)m \tag{2}$$

where:

Q_c' = rate of heat transfer from cooling coils

m = mass flow rate of refrigerant

h_1 = enthalpy of refrigerant leaving cooling coils

h_2 = enthalpy of refrigerant entering expansion valve

Refrigerant flow rate, m, is measured with a flow meter. Enthalpy leaving coils, h_1, is calculated from measured temperature and pressure of refrigerant at a point down line from the cooling coils. Refrigerant at this location is assumed to be a superheated vapor. Enthalpy entering expansion valve, h_2, is calculated from the measured temperature of refrigerant entering the expansion valve. Refrigerant at this location is assumed to be a saturated liquid.

Deviation from the ideal vapor cycle may result from a combination of heat transfer through finite temperature differences, irreversible adiabatic compression, and pressure losses in the evaporator and condenser.[11] In addition, refrigerant entering the expansion valve may not be saturated liquid.

Adjustments made to compensate for inefficiencies in the actual cycle are based on steady-state calibrated hot box test results for the two "standard" calibration specimens. Results indicate that inefficiencies are linearly related to refrigerant flow rate and the air temperature of the indoor chamber. For Wall C2 a reference efficiency was established based on particular values of refrigerant flow rate and the indoor chamber air temperature. The heat removed from indoor chamber cooling, Q_c, was determined from values of Q_c' adjusted to consider changes in efficiencies from the reference values.

Laboratory Losses

Heat losses or gains from the laboratory to the indoor chamber, Q_ℓ, are calculated based on thermal properties of component materials making up walls and ceilings of the indoor chamber and temperature conditions on the inner and outer surfaces of the indoor chamber. Two heat flux transducers mounted on the inside surface of the indoor chamber are used as a check on calculated laboratory losses. One heat flux transducer is mounted on the ceiling and one is mounted on a wall.

For steady-state and dynamic tests performed on Wall C2, the indoor chamber air and laboratory air temperatures were maintained at the same nominal value, 72°F (22°C), to minimize laboratory losses. Thus, the value of Q_ℓ is small relative to other terms of the energy balance equation.

Flanking Losses

Heat loss or gain from flanking around the test specimen, Q_f, is determined from steady-state tests of standard calibration walls. The flanking loss Q_f can be determined from Eq. (1) when all other terms in the equation are known. Since thermal conductance of each standard calibration wall is known, Q_w for a given steady-state test can be calculated using the following equation:

$$Q_w = \frac{A \cdot C \cdot (t_2 - t_1)}{3.413} \tag{3}$$

where:

Q_w = heat transfer through test wall, W·hr/hr

A = area of wall surface normal to heat flow, ft^2

C = average thermal conductance, $Btu/hr \cdot ft^2 \cdot °F$

t_2 = average temperature of outside wall surface, °F

t_1 = average temperature of inside wall surface, °F

3.413 = conversion factor from W·hr/hr to Btu/hr

Thus, Q_f can be determined from Eq. (1) using calculated values of Q_w, Q_c, and Q_ℓ, and measured values of Q_h and Q_{fan}.

For both standard calibration walls, values of Q_f were observed to follow the relationship:

$$Q_f = 0.235\ (t_2 - t_1) \tag{4}$$

where:

Q_f = heat loss or gain from flanking around test specimen, W·hr/hr

t_2 = average temperature of outside wall surface, °F

t_1 = average temperature of inside wall surface, °F

Since Q_f is the residual from Eq. (1), it may include other undetermined losses from the indoor chamber.[10]

THERMAL PROPERTIES OF CONCRETE UNDER STEADY-STATE CONDITIONS

Thermal conductivity and thermal transmittance of Wall C2 were derived from steady-state tests using the calibrated hot box. Specific heat, thermal conductivity, and thermal diffusivity were also obtained from tests performed on control specimens.

Specific Heat

Specific heats of concrete control specimens and constituent aggregates were measured using a method similar to U.S. Army Corps of Engineers Specification CRD-C124-73, "Method of Test for Specific Heat of Aggregates, Concrete, and Other Materials (Method of Mixtures)."[12] The concrete test sample was selected from pulverized parts of five 3x6-in. (76x152-mm) cylinders cured one day in molds, and then 27 days at 73±3°F (23±1.7°C) and 100% RH.

Test Method

To determine specific heat, samples of crushed material were heated in a warm bath at 115±1°F (46.1±0.6°C) and then transferred to a calorimeter containing room temperature water. After acquiring necessary data, the sample was then cooled in water at 35°F (2°C) and again transferred to the calorimeter. The specific heat was found by measuring the temperature change of the water in the calorimeter.

Since this is a wet method, the specific heat determined is that of the saturated material. To determine specific heat of the material in a dry state, weights of the material in the particular dry state, and the saturated surface dry (SSD)* state must be known.

Whiting, Litvin, and Goodwin[13] used the following equation to calculate specific heat of concrete for various moisture conditions:

$$c = \frac{c_{SSD} + \gamma(y-1)}{1 + \gamma(y-1)} \tag{5}$$

where:

c = specific heat of samples at any moisture content

c_{SSD} = specific heat of saturated surface dry samples

y = moisture content expressed as a fraction of the SSD moisture content

γ = SSD moisture content

$$\gamma = \frac{W_{SSD} - W_{OD}}{W_{SSD}} \tag{6}$$

where:

W_{SSD} = SSD weight of sample

W_{OD} = ovendry weight of sample

Results

Measured values of specific heat for concrete and constituent aggregates of Wall C2 are shown in Table 8. Specific heat of the aggregates is less than the specific heat of structural lightweight concrete.

*A SSD material is a saturated material with surface water removed.

TABLE 8 - SPECIFIC HEAT OF CONCRETE AND CONSTITUENT AGGREGATES

Description	SSD Moisture Content, % ovendry weight	SSD Specific Heat, Btu/lb·°F (J/kg·°K)
Wall C2 Concrete	12.3	0.257 (1080)
Expanded Shale Aggregate	7.0	0.198 (830)

Data for specific heat are compared with results from Whiting, Litvin, and Goodwin[13] in Table 9. Values are for lightweight concrete in saturated surface dry, air dry, and ovendry conditions. Aggregates for Wall C2 and Whiting Mix No. 4 were expanded shale. Concrete for Whiting Mix No. 3 contained expanded shale as coarse aggregate and sand as fine aggregate.

Specific heats in the air dry and ovendry conditions were calculated using Eqs. (5) and (6). Differences in air dry moisture contents of concretes given in Table 9 are due to methods of determining moisture content. Air dry moisture content of Wall C2 was measured as explained in the subsection "Moisture Content" of the "Physical Properties of Concrete" section. Whiting, Litvin, and Goodwin estimated air dry moisture contents using a relationship between moisture content and unit weight proposed by Brewer.[13]

Thermal Conductivity

The guarded hot plate (ASTM Designation: C177) and hot wire methods were used to determine thermal conductivity of Wall C2 control specimens. Thermal conductivity of Wall C2 was derived using steady-state calibrated hot box tests.

Guarded Hot Plate

Average apparent thermal conductivity of two 5.6x5.6x2.00 -in. (142x142x50.7-mm) prisms was determined in accordance with ASTM Designation: C177, "Standard Test Method for Steady-State Thermal Transmission Properties by Means of the Guarded Hot Plate"[8] at Dynatech R/D Company in Cambridge, Mass.[14] Specimens were

TABLE 9 SPECIFIC HEAT OF LIGHTWEIGHT CONCRETE

Specimen	Saturated Surface Dry			Air Dry			Ovendry	
	Unit Weight, pcf (kg/m^3)	Moisture Content, % ovendry weight	Specific Heat, Btu/lb·°F (J/kg·°K)	Unit Weight, pcf (kg/m^3)	Moisture Content, % ovendry weight	Specific Heat, Btu/lb·°F (J/kg·°K)	Unit Weight, pcf (kg/m^3)	Specific Heat, Btu/lb·°F (J/kg·°K)
Whiting:[13] Mix No. 4	98 (1570)	15.3	0.311 (1300)	88 (1410)	3.5	0.227 (950)	85 (1360)	0.203 (850)
Wall C2	106 (1700)	12.3	0.257 (1080)	102 (1630)	8.5	0.230 (960)	94 (1510)	0.162 (680)
Whiting:[13] Mix No. 3	118 (1890)	10.3	0.275 (1150)	109 (1750)	2.8	0.216 (904)	106 (1700)	0.199 (833)

cured for seven days in molds and approximately one year at 73±5°F (23±3°C) and 45±15% RH. Samples were cut to size from two 16x16x2-in. (406x406x51-mm) specimens. Both prisms were ovendried prior to testing.

In standard practice, thermocouples are placed on the surface of test specimens. For tests conducted at Dynatech R/D Company, thermocouples were embedded into two surfaces of each specimen. Fine wire thermocouples in silica protective tubes were fitted tightly into 0.020x0.020-in. (0.51x0.51-mm) grooves that had been cut into the surfaces. According to Tye & Spinney[15] if thermocouples are not embedded in the specimen, a contact resistance may be introduced between the thermocouple junction and the concrete surface. This will result in an artificially large temperature difference across the specimen. Consequently, the derived value of conductivity will be too low.[15]

Apparent thermal conductivity of ovendry samples obtained by hot plate test at a mean specimen temperature of 70°F (21°C) was 4.5 Btu·in./hr·ft^2·°F (0.65 W/m·°K).

Hot Wire Method

The hot wire method was used to determine apparent thermal conductivity of air dry and ovendry prisms. Concrete prisms were cast with a nickel-chromium constantan thermocouple embedded along their central longitudinal axis. Figure 13 shows a mold for the 4x4x8-in. (102x102x204-mm) prisms.

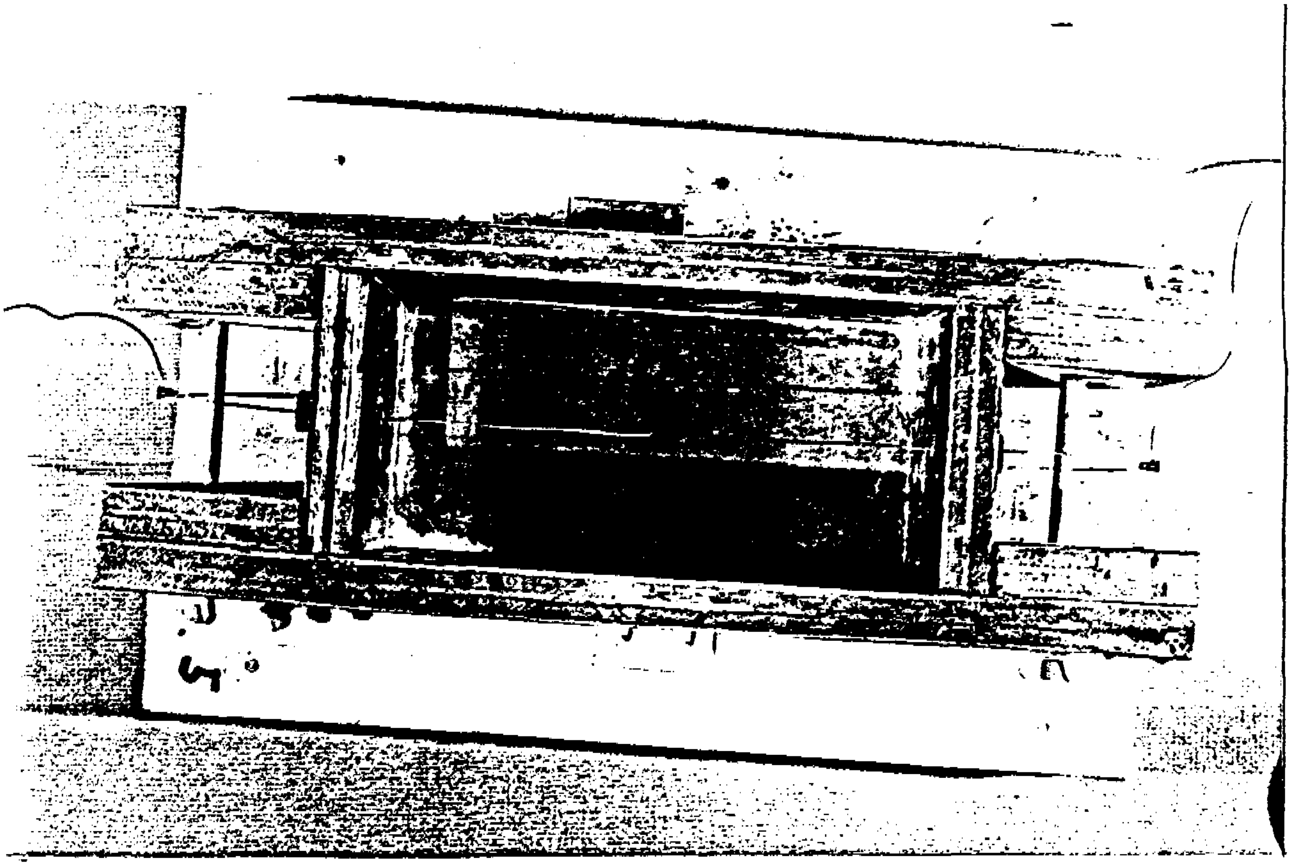

Fig. 13 Mold for Hot Wire Conductivity Specimen with Embedded Thermocouple

To test a specimen using the hot wire method, a thermocouple reading is taken, electrical current is supplied to the wire, and additional temperature readings are made at selected intervals for a period of ten minutes. Apparent thermal conductivity is calculated from the measured current, the resistance of the wire, and the thermocouple readings.(16)

Thermal conductivity was measured for two sets of specimens. A first set of three specimens was cured in molds for seven days, and then air cured at 73±5°F (23±3°C) and 45±15% RH for 91 days. Conductivity of these specimens was determined for the air dry and ovendry conditions.

A second set of three specimens was cured in molds for 24 hours, and then moist cured at 73±3°F (23±1.7°C) and 100% RH for 119 days. Specimens were first tested immediately after removal from the moist cure room. Tests were then conducted after specimens had been air dried for 7, 26, and 54 days. A final test was performed on specimens after they had been ovendried.

Average apparent thermal conductivity for air cured specimens in the air dry condition was 6.0 Btu·in./hr·ft^2·°F (0.87 W/m·°K). Average apparent thermal conductivity for ovendry air cured specimens was 4.2 Btu·in./hr·ft^2·°F (0.61 W/m·°K). Hot wire test results for the three moist cured samples are shown in Table 10. Each moist cured specimen was tested at five different moisture contents.

Calibrated Hot Box

Apparent thermal conductivity of concrete in Wall C2 can also be derived from steady-state calibrated hot box tests.

TABLE 10 - THERMAL CONDUCTIVITY AT DIFFERENT MOISTURE CONTENTS OF CONCRETE FOR WALL C2, HOT WIRE METHOD

Length of Time Air Cured,* days	Moisture Content, % ovendry weight	Unit Weight, pcf (kg/m^3)	Moisture Content, % volume	k Thermal Conductivity, $\frac{Btu \cdot in.}{hr \cdot ft^2 \cdot °F}$ ($W/m \cdot °K$)	$\frac{k_{(moist)}}{k_{(ovendry)}}$
63**	0	93 (1490)	0	5.14 (0.740)	1.00
54	9.5	102 (1630)	14.1	6.85 (0.987)	1.33
26	10.5	103 (1650)	15.7	7.02 (1.012)	1.37
7	11.6	104 (1660)	17.3	6.98 (1.007)	1.36
0	13.6	106 (1700)	20.2	9.91 (1.429)	1.93

*All specimens cured 24 hours in molds and 119 days at 73±3°F (23±1.7°C) and 100% RH prior to air curing.
**Ovendry

Steady-state tests are conducted by maintaining constant indoor and outdoor chamber temperatures.

Results are calculated from data collected when specimen temperatures reach equilibrium and the rate of heat flow through the test wall is constant.

Since thermal conductivity is equal to conductance times wall thickness, Eq. (3) can be modified as follows:

$$k = \frac{3.413 \cdot t \cdot Q_w}{A \cdot (t_2 - t_1)} \tag{7}$$

where:

k = thermal conductivity, $Btu \cdot in./hr \cdot ft^2 \cdot {}^\circ F$

t = wall thickness, in.

Q_w = heat transfer through test wall, $W \cdot hr/hr$

A = area of wall surface normal to heat flow, ft^2

t_2 = average temperature of outside wall surface, °F

t_1 = average temperature of inside wall surface, °F

3.413 = conversion factor from $W \cdot hr/hr$ to Btu/hr

Thermal conductivity was determined from steady-state test data using Eq. (7). The amount of heat passing through the test wall, Q_w, was calculated from Eq. (1).

Values of conductivity are reported in Table 11 for four different mean wall temperatures. Mean wall temperature is the average of the indoor wall surface temperature, t_1, and the outdoor wall surface temperature, t_2.

Discussion of Results

An increase in moisture content of concrete increases its conductivity. Figure 14 shows the ratio of conductivity of

TABLE 11 - THERMAL CONDUCTIVITY DERIVED FROM CALIBRATED HOT BOX STEADY-STATE TEST RESULTS OF WALL C2

Mean Wall Temperature, °F (°C)	Thermal Conductivity, $\frac{Btu \cdot in.}{hr \cdot ft^2 \cdot °F}$ (W/m·°K)
33.9 (1.1)	4.66 (0.672)
51.9 (11.1)	4.69 (0.676)
87.7 (30.9)	4.77 (0.688)
99.0 (37.2)	4.83 (0.696)

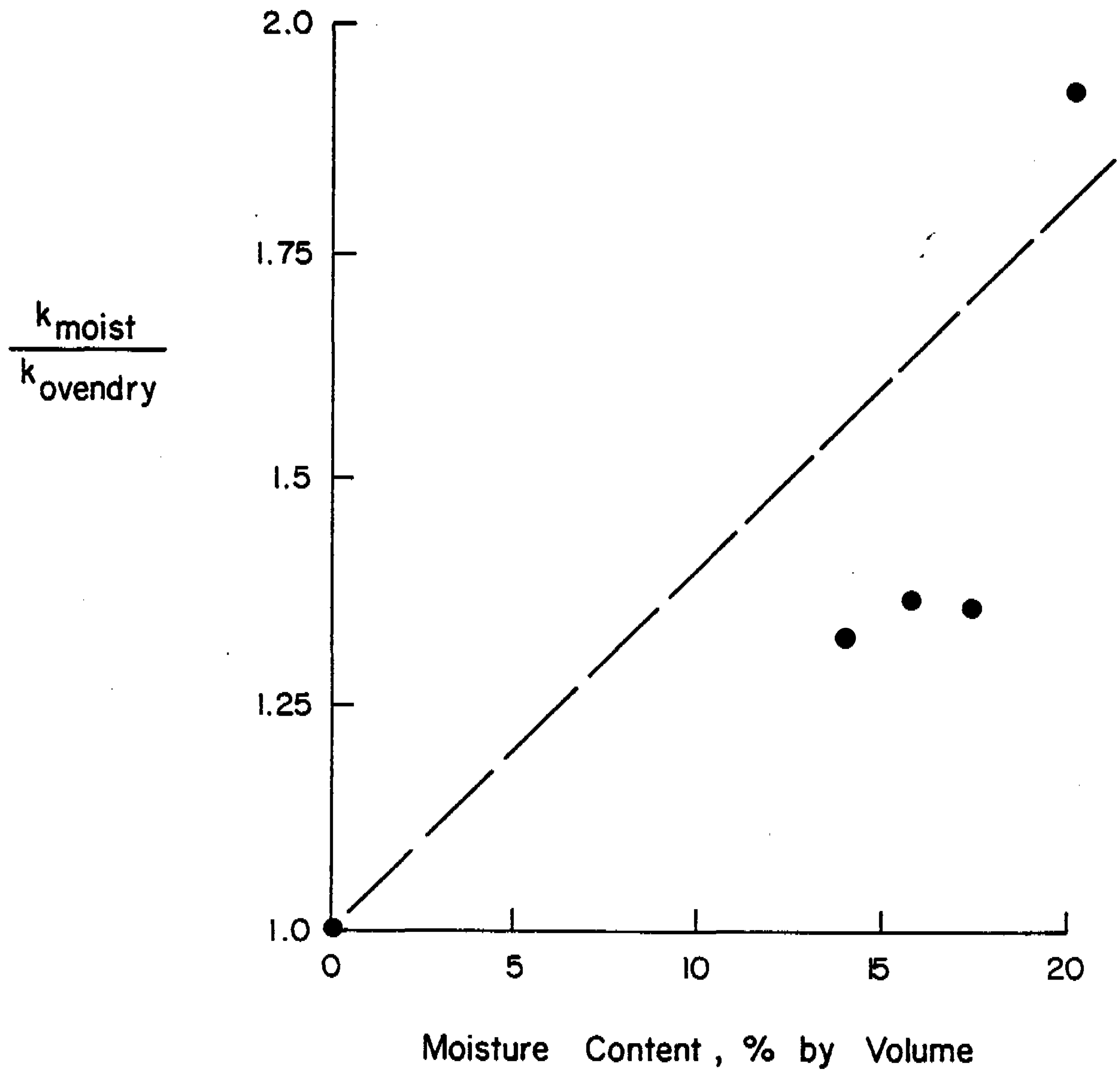

Fig. 14 Thermal Conductivity of Structural Lightweight Concrete as a Function of Moisture Content

lightweight concrete at a particular moisture content to conductivity of the ovendry concrete plotted as a function of moisture content. Data were obtained from hot wire tests of moist cured specimens, and are listed in Table 10. The broken line shown in the figure is based on the assumption that a 5% increase in moisture content leads to a 20% increase in thermal conductivity over the ovendry value.(17) Three of four data points shown in Fig. 14 show a smaller increase in conductivity with moisture content than is predicted by the assumed relationship.

Results from calibrated hot box tests indicate an increase in thermal conductivity of lightweight concrete with temperature. Figure 15 shows thermal conductivity as a function of mean wall temperature. Data were obtained from steady-state calibrated hot box tests of Wall C2 and are listed in Table 11.

The following equations have been used to estimate thermal conductivity of ovendry and air dry concrete:(18)

Ovendry:

U.S. units $k = 0.5e^{0.02\rho}$ (8)

S.I. units $k = 0.072e^{1250\rho}$

Air Dry:

U.S. units $k = 0.6e^{0.02\rho}$ (9)

S.I. units $k = 0.0865e^{1250\rho}$

where:

k = thermal conductivity, Btu·in./hr·ft^2·°F (W/m·°K)

ρ = ovendry unit weight of concrete, pcf (kg/cm^3)

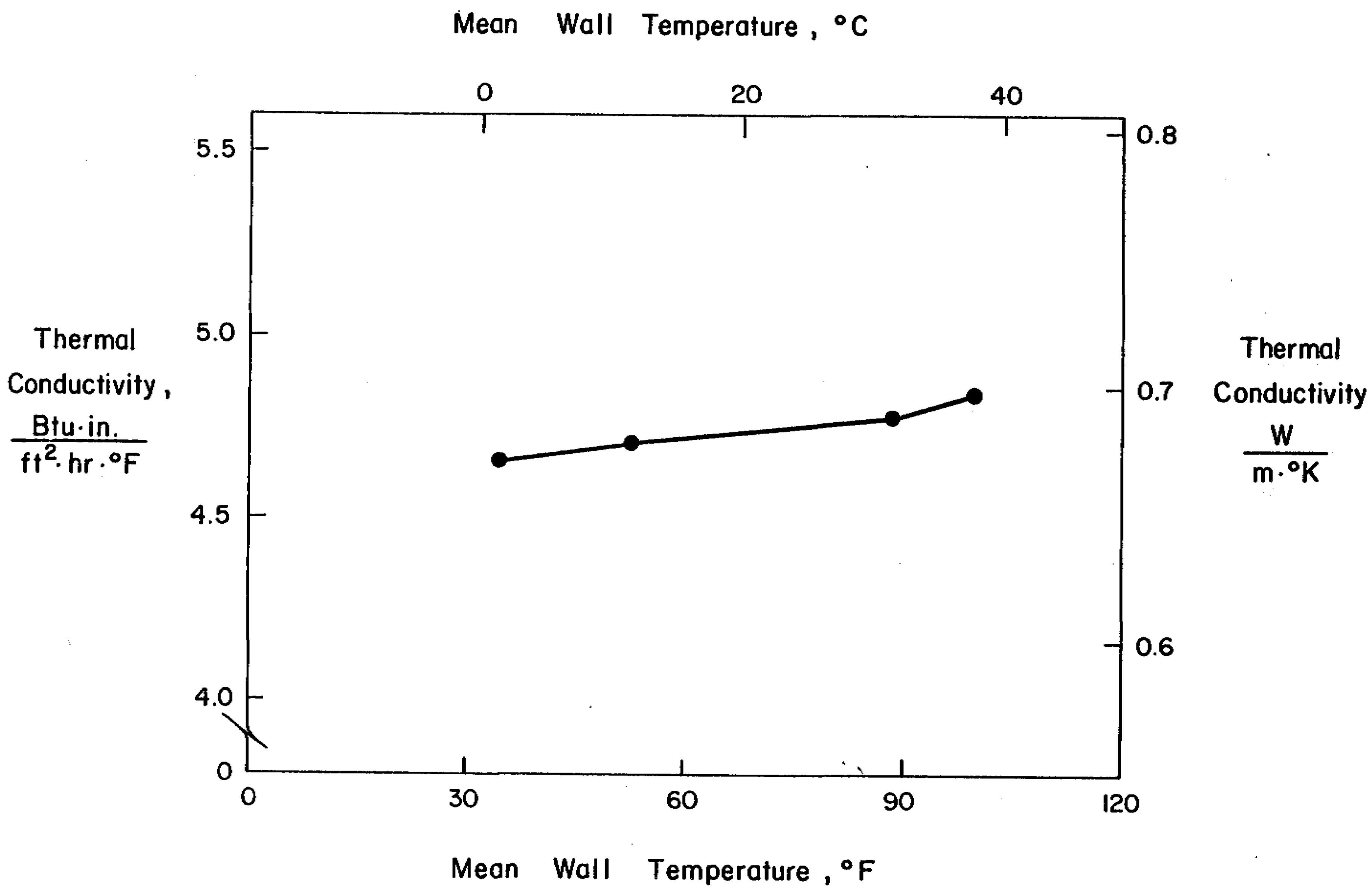

Fig. 15 Thermal Conductivity of Structural Lightweight Concrete as a Function of Temperature

Estimated values of thermal conductivity calculated from Eqs. (8) and (9) are given in Table 12. The ovendry unit weight of Wall C2 was taken to be 94 pcf (1510 kg/m^3).

Table 12 shows that estimated values of conductivity are less than measured values for the lightweight concrete. Measured values of ovendry lightweight concrete determined using the guarded hot plate and hot wire method are greater than the estimated value. The measured value of air dry lightweight concrete determined from the hot wire method is considerably greater than the value calculated from Eq. (9). Results from calibrated hot box tests are 20% greater than the estimated value.

Results from hot wire and Dynatech guarded hot plate tests may be greater than results from calibrated hot box tests and estimated values because of contact resistance temperature measurement error.[15] This error is due to the influence of any thin air gap between the thermocouple wire and the lightweight concrete at their point of contact. This additional thermal resistance can be introduced when thermocouples are not embedded in the test material. Contact resistance is a larger portion of the total resistance for materials with larger thermal conductivities.[15]

The calibrated hot box test, with thermocouples taped to the concrete surface, produced apparent thermal conductivity results which were lower than results determined using the hot wire method, with embedded thermocouples. These results are indicative of a contact resistance in the determination of

TABLE 12 - THERMAL CONDUCTIVITY OF WALL C2

Test Method or Equation	Thermal Conductivity,* $\frac{\text{Btu}\cdot\text{in.}}{\text{hr}\cdot\text{ft}^2\cdot{}^\circ\text{F}}$ ($\text{W/m}\cdot{}^\circ\text{K}$)	
	Ovendry Concrete	Air Dry Concrete
Guarded Hot Plate, ASTM Designation: C177**	4.5 (0.65)	--
Hot Wire Method	4.2 (0.61)	6.0 (0.87)
Calibrated Hot Box, ASTM Designation: C976	--	4.7 (0.68)
Estimated using Eq. (8)	3.3 (0.47)	--
Estimated using Eq. (9)	--	3.9 (0.57)

*For 70°F mean temperature of specimen
**Specimens cured in molds for seven days, then air cured

apparent thermal conductivity using the calibrated hot box. Thermocouple wires were applied to Wall C2 in accordance with ASTM Designation: C976, Section 5.7.1, which states that requirements of the standard are presumed to be met if wire is "taped, cemented or otherwise held in thermal contact with the surface using materials of emittance close to that of the surface."(8)

Thermal Diffusivity

Thermal diffusivity was determined using 6x12-in. concrete cylinders according to U.S. Army Corps of Engineers Specification CRD-C36-73, "Method of Test for Thermal Diffusivity of Concrete."(19) Test specimens were cured in their molds for 24 hours, and then moist cured at 73±3°F (23±1.7°C) and 100% RH for 74 days. Measured thermal diffusivity was 0.0155 ft^2/hr (0.400 mm^2/s) for the saturated lightweight concrete.

Thermal diffusivity can also be calculated from the following formula:

$$\alpha = \frac{k}{\rho \cdot c} \tag{10}$$

where:

α = thermal diffusivity, ft^2/hr (m^2/s)

k = thermal conductivity, Btu/hr·ft·°F (W/m·°K)

ρ = unit weight, pcf (kg/m^3)

c = specific heat, Btu/lb·°F (J/kg·°K)

If any three of the values of conductivity, specific heat, unit weight, or diffusivity are known, the fourth can be calculated.

Since measured values of diffusivity and specific heat are for saturated specimens, conductivity and unit weight used in Eq. (10) should also be for saturated specimens.

Calculated thermal diffusivity of saturated concrete for Wall C2 is 0.0307 ft^2/hr (0.792 mm^2/s). Results from hot wire tests of specimens with an average moisture content of 13.6% by weight were used as input to Eq. (10). This moisture content was within 10% of the SSD moisture content determined using specific heat tests.

Thermal diffusivity of air dry lightweight "clinker" concrete measured by Billington[20] was 0.018 ft^2/hr (0.46 mm^2/s). Unit weight of the air cured concrete was 108 pcf (1730 kg/m^3). Billington measured diffusivity by alternately heating and cooling test specimens. The temperature history of each specimen was used to calculate diffusivity.[20]

For Wall C2, calculated diffusivity is 98% greater than the measured value. Measured diffusivity of Wall C2 is 16% greater than diffusivity measured by Billington.[20]

Thus, it appears that test methods for conductivity, specific heat, and diffusivity of concrete do not correlate well with theoretical expectations. This may be attributed to differing effects of moisture on each particular test procedure.

Thermal Transmittance

Total thermal resistance (R_T) and thermal transmittance (U) values for the four mean wall temperatures used in the calibrated hot box tests are listed in Table 13. Overall coefficients were obtained by correcting measured data obtained from

TABLE 13 - TOTAL THERMAL RESISTANCE (R_T) AND THERMAL TRANSMITTANCE (U) VALUES FOR STRUCTURAL LIGHTWEIGHT CONCRETE WALL C2

Mean Wall Temperature, °F (°C)	R_T, $\frac{hr \cdot ft^2 \cdot °F}{Btu}$ ($m^2 \cdot °K/W$)	U, $\frac{Btu}{hr \cdot ft^2 \cdot °F}$ ($W/m^2 \cdot °K$)
33.9 (1.1)	2.63 (0.463)	0.38 (2.2)
51.9 (11.1)	2.62 (0.461)	0.38 (2.2)
87.7 (30.9)	2.59 (0.456)	0.39 (2.2)
99.0 (37.2)	2.56 (0.451)	0.39 (2.2)

steady-state calibrated hot box tests to account for standard surface resistance coefficients. Surface resistances were taken as 0.68 hr·ft^2·°F/Btu (0.12°K·m^2/W) for inside and 0.17 hr·ft^2·°F/Btu (0.03°K·m^2/W) for outside. These values are commonly used in design and are considered to represent still air on the inside and an air flow of 15 mph (24 km/hr) on the outside.

Steady-State Temperature Profiles

Temperature profiles of all steady-state tests with a temperature differential across the wall significantly different from zero are illustrated in Figs. 16 through 19. The following notation is used to designate average measured temperatures:

t_i = indoor chamber air temperature

t_1 = wall surface temperature, indoor side

t_3 = internal wall temperature at approximate midthickness

t_2 = wall surface temperature, outdoor side

t_o = outdoor chamber air temperature

Theoretically, the slope of the temperature profile line through a homogeneous wall should be constant. As can be seen from Figs. 18 and 19, the slopes of lines through Wall C2 joining t_2 to t_3 and t_3 to t_1 are not exactly equal. This may be due to two factors. First, the location of thermocouple t_3 may not be exactly 4 in. from the inside surface of Wall C2. Secondly, the contact resistance measurement error, described in the section on thermal conductivity, may affect surface temperatures in a manner that alters the apparent temperature profile from the true temperature profile.

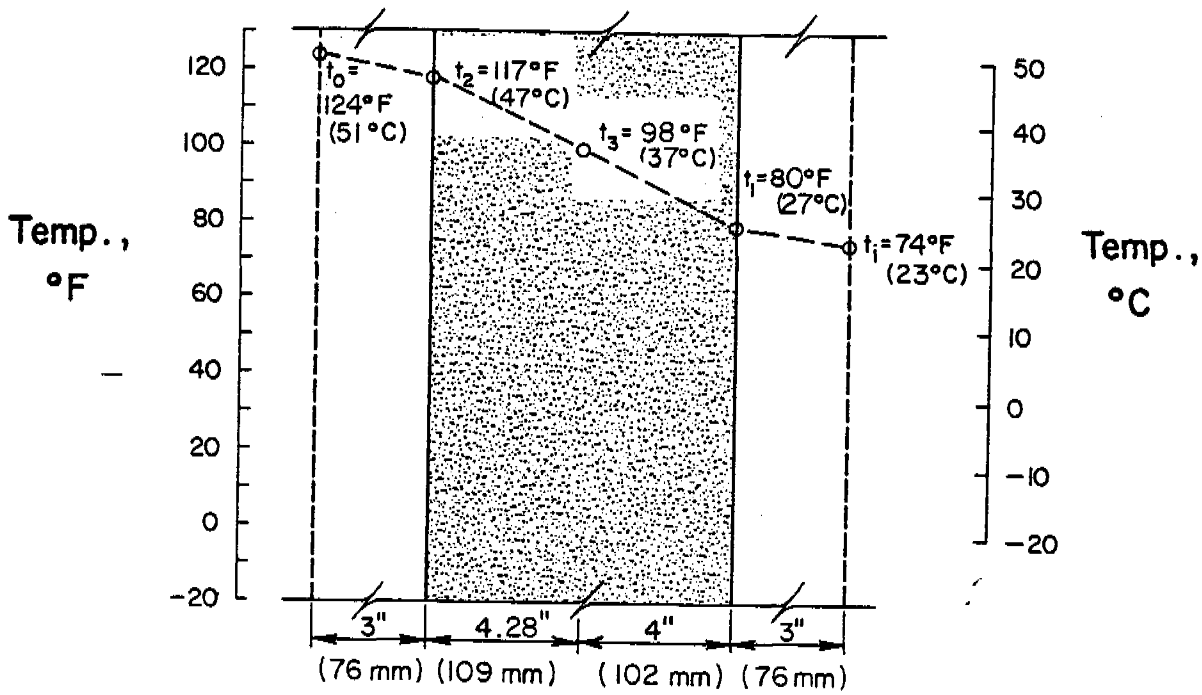

Fig. 16 Temperature Profile Across Wall C2, Mean Wall Temperature = 99°F (37°C)

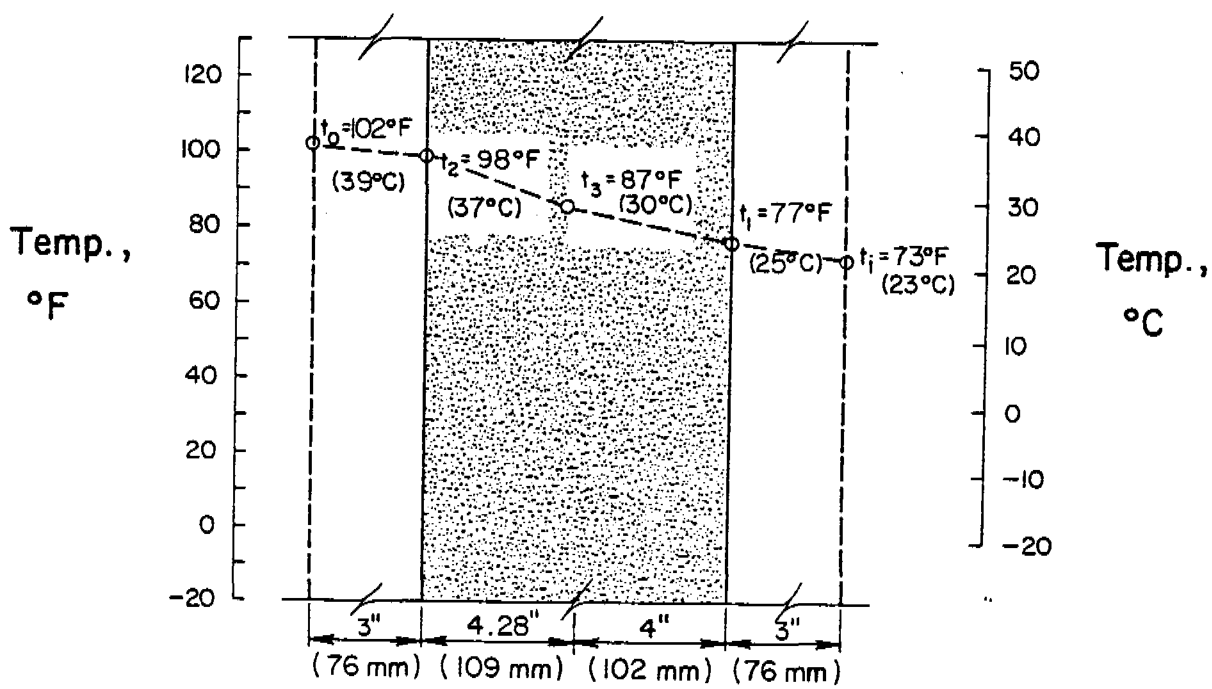

Fig. 17 Temperature Profile Across Wall C2, Mean Wall Temperature = 88°F (31°C)

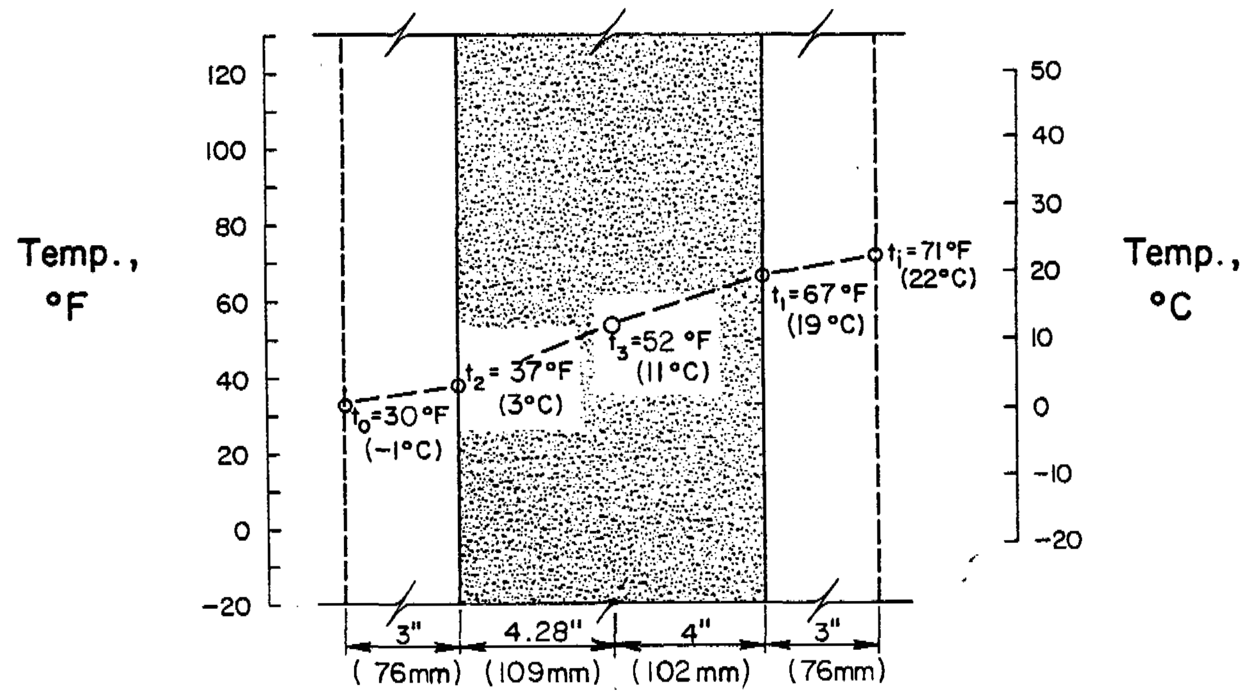

Fig. 18 Temperature Profile Across Wall C2, Mean Wall Temperature = 52°F (11°C)

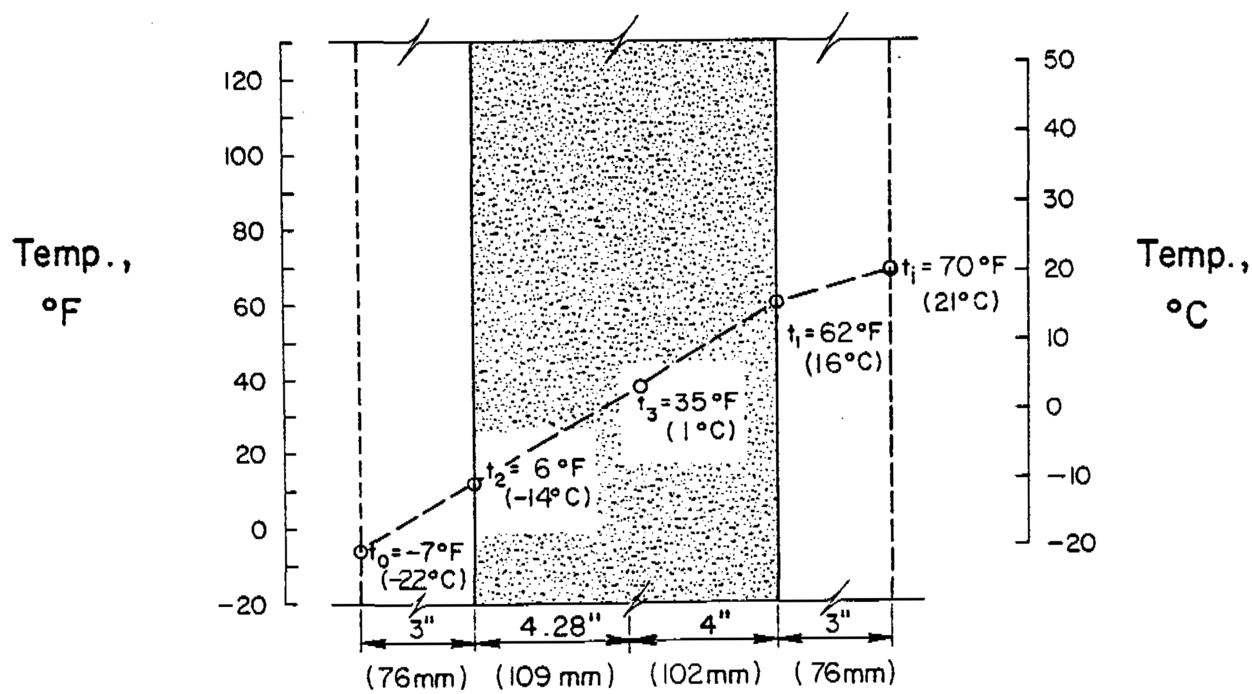

Fig. 19 Temperature Profile Across Wall C2, Mean Wall Temperature = 34°F (1°C)

THERMAL PROPERTIES OF CONCRETE UNDER DYNAMIC TEST CONDITIONS

Although steady-state tests provide a measure of resistance to heat flow, response of walls to temperature changes is a function of both thermal resistance and heat storage capacity. Dynamic tests are a means of evaluating thermal response under controlled conditions that simulate temperature changes actually encountered in building envelopes. These tests provide a comparative measure of response and also can be used to verify analytical models for transient heat flow.

Test Procedure

Dynamic tests were conducted by maintaining calibrated hot box indoor air temperatures constant while outdoor air temperatures were cycled over a predetermined time versus temperature relationship. Energy required to maintain a constant indoor air temperature was monitored as a function of time. The rate of heat flow through Wall C2 was determined using Eq. (1) for hourly averages of data.

Three 24-hour (diurnal) temperature cycles were used in this investigation. The first cycle applied to Wall C2 was based on a simulated sol-air* cycle used by the National Bureau of Standards in their evaluation of dynamic thermal performance of an experimental masonry building.[21] It represents a large variation in outdoor temperature over a 24-hour period. The mean

*Sol-air temperature is that temperature of outdoor air that, in the absence of all radiation exchanges, would give the same rate of heat entry into the surface as would exist with the actual combination of incident solar radiation, radiant energy exchange, and convective heat exchange with outdoor air.[11]

outdoor temperature of the cycle was approximately equal to the mean indoor temperature. This cycle, denoted NBS, was run to permit comparison of results with those from earlier tests.[1-3]

Two additional sol-air temperature cycles were run with mean outdoor temperatures approximately 10°F (6°C) above and 10°F (6°C) below the indoor temperature. The NBS+10 cycle was derived by increasing hourly outdoor temperatures of the NBS cycle by 10°F (6°C). The NBS-10 cycle was derived by decreasing hourly outdoor temperatures by 10°F (6°C).

Outdoor chamber air temperatures for the three test cycles are illustrated in Fig. 20. Average indoor temperature over the 24-hour period for each dynamic cycle was approximately 72°F (22°C). This is shown as a reference line in Fig. 20. Plotted temperatures were recorded in the air plenum of the outdoor and indoor chambers.

For all tests, dynamic cycles were repeated until conditions of equilibrium were obtained. Equilibrium conditions were evaluated by consistency of applied temperatures and measured energy response. Each test required approximately four to six days for completion. After equilibrium conditions were reached, the test was continued for a period of three days. Results are based on average readings for at least three consecutive 24-hour cycles.

Dynamic Test Results

Results for the three diurnal tests are given in Tables 14 through 17 and Figs. 21 through 29. Tables 14 through 16 and Figs. 21, 24, and 27 give measured air, surface, and internal

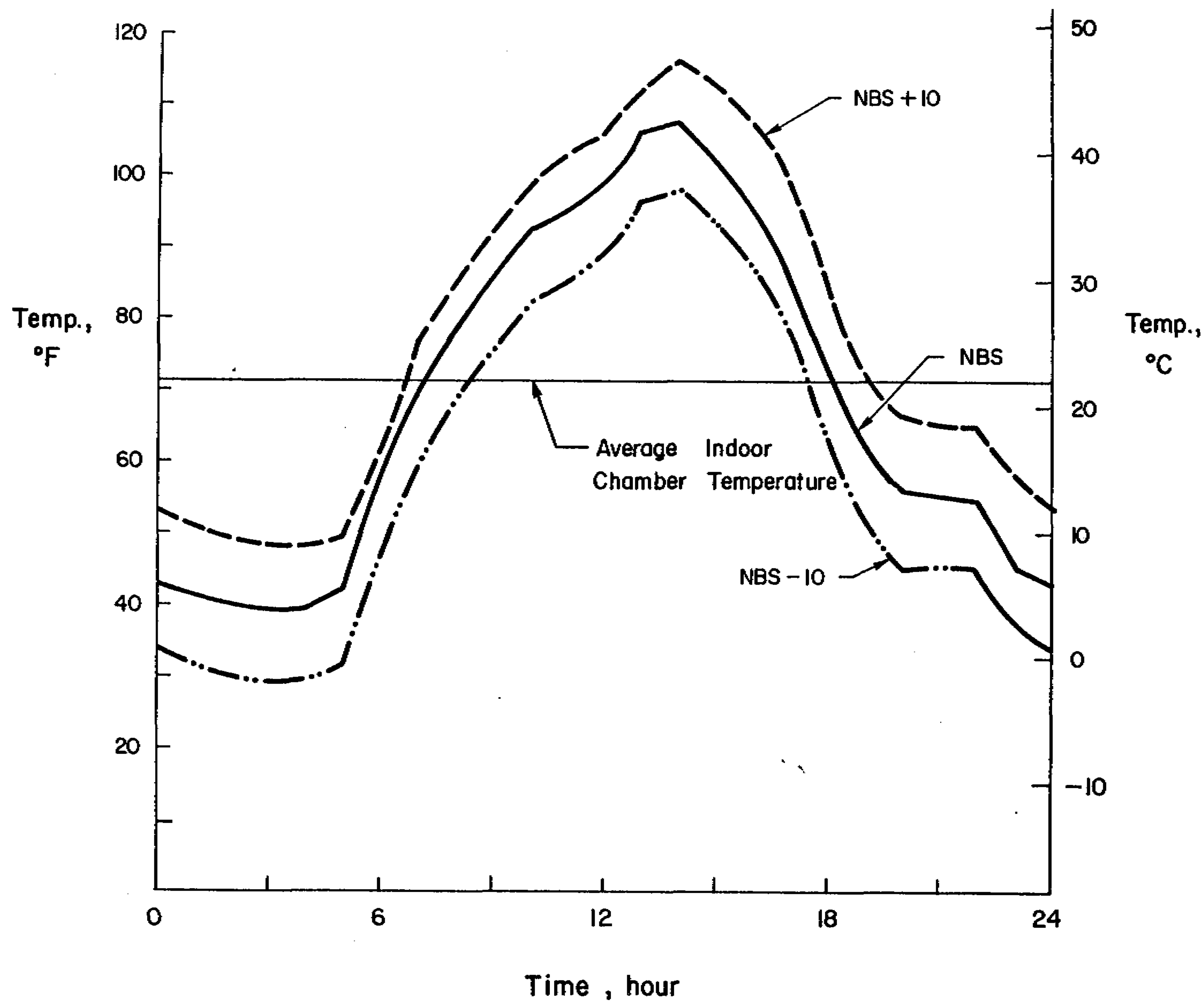

Fig. 20 Outdoor Chamber Air Temperatures for Dynamic Test Cycles

TABLE 14 - MEASURED TEMPERATURES OF WALL C2 FOR NBS TEST CYCLE

Time, hr	Outdoor Chamber Air Temperature, t_o		Outdoor Surface Temperature of Wall, t_2		Internal Wall Temperature, t_3		Indoor Surface Temperature of Wall, t_1		Indoor Chamber Air Temperature, t_i	
	°F	°C	°F	°C	°F	°C	°F	°C	°F	°C
1	44.18	6.77	54.10	12.28	69.70	20.94	72.50	22.50	72.13	22.30
2	42.11	5.62	52.22	11.23	68.35	20.19	72.10	22.28	72.04	22.24
3	41.17	5.09	50.92	10.51	67.05	19.47	71.71	22.06	71.94	22.19
4	40.85	4.92	50.11	10.06	65.87	18.82	71.32	21.84	71.87	22.15
5	41.06	5.03	49.67	9.82	64.78	18.21	70.95	21.64	71.77	22.09
6	50.06	10.03	53.62	12.01	63.87	17.71	70.61	21.45	71.73	22.07
7	62.27	16.82	60.78	15.99	63.37	17.43	70.28	21.27	71.71	22.06
8	70.30	21.28	66.43	19.13	63.58	17.54	70.05	21.14	71.65	22.03
9	77.13	25.07	71.47	21.93	64.29	17.94	69.96	21.09	71.64	22.02
10	83.52	28.62	76.25	24.58	65.35	18.53	70.05	21.14	71.64	22.02
11	88.02	31.12	80.26	26.81	66.73	19.29	70.27	21.26	71.70	22.06
12	91.05	32.81	83.17	28.43	68.31	20.17	70.65	21.47	71.76	22.09
13	96.96	36.09	87.36	30.76	69.89	21.05	71.06	21.70	71.90	22.17
14	100.91	38.28	91.10	32.83	71.58	21.99	71.50	21.94	72.00	22.22
15	98.56	36.98	91.10	32.83	73.21	22.89	71.96	22.20	72.03	22.24
16	94.13	34.52	89.22	31.79	74.73	23.74	72.44	22.47	72.15	22.31
17	86.35	30.19	85.14	29.52	75.88	24.38	72.91	22.73	72.23	22.35
18	73.99	23.33	78.02	25.57	76.41	24.67	73.31	22.95	72.31	22.39
19	64.20	17.89	71.22	21.79	76.31	24.62	73.60	23.11	72.38	22.43
20	58.80	14.89	66.72	19.29	75.61	24.23	73.71	23.17	72.39	22.44
21	57.01	13.89	64.40	18.00	74.54	23.63	73.66	23.14	72.39	22.44
22	56.52	13.62	63.27	17.37	73.37	22.98	73.44	23.02	72.33	21.41
23	50.08	10.04	59.54	15.30	72.27	22.37	73.16	22.87	72.28	22.38
24	45.47	7.48	55.80	13.22	71.05	21.69	72.84	22.69	72.19	22.33

TABLE 15 - MEASURED TEMPERATURES OF WALL C2 FOR NBS+10 TEST CYCLE

Time, hr	Outdoor Chamber Air Temperature, t_o		Outdoor Surface Temperature of Wall, t_2		Internal Wall Temperature, t_3		Indoor Surface Temperature of Wall, t_1		Indoor Chamber Air Temperature, t_i	
	°F	°C	°F	°C	°F	°C	°F	°C	°F	°C
1	52.86	11.59	61.27	16.26	73.89	23.21	73.92	23.29	72.62	22.57
2	51.11	10.62	59.46	15.26	72.59	22.55	73.56	23.09	72.58	22.54
3	50.12	10.07	58.23	14.57	71.31	21.84	73.17	22.87	72.47	22.48
4	50.56	10.31	57.78	14.32	70.11	21.17	72.79	22.66	72.41	22.45
5	51.78	10.99	57.94	14.41	69.03	26.57	72.43	22.46	72.28	22.38
6	62.73	17.07	63.14	17.30	68.21	20.12	72.09	22.27	72.29	22.38
7	74.27	23.48	70.46	21.37	67.86	19.92	71.81	22.12	72.24	22.36
8	81.50	27.50	75.80	24.33	68.16	20.09	71.61	22.01	72.17	22.32
9	87.23	30.68	80.14	26.74	68.82	20.46	71.41	21.89	72.07	22.26
10	93.48	34.16	84.83	29.35	70.01	21.12	71.52	21.96	72.10	22.28
11	97.19	36.22	88.35	31.31	71.43	21.91	71.77	22.09	72.16	22.31
12	100.59	38.11	91.33	32.96	73.00	22.78	72.13	22.29	72.28	22.38
13	106.33	41.29	95.66	35.37	74.51	23.62	72.53	22.52	72.36	22.42
14	108.87	42.71	98.69	37.05	76.20	24.56	73.00	22.78	72.50	22.50
15	106.04	41.13	98.22	36.79	77.79	25.44	73.48	23.04	72.55	22.53
16	101.80	38.78	96.20	35.67	79.26	26.26	74.00	23.33	72.66	22.59
17	93.99	34.44	92.03	33.35	80.33	26.85	74.42	23.57	72.75	22.64
18	80.85	27.14	84.37	29.09	80.82	27.12	74.82	23.79	72.83	22.68
19	71.51	21.95	77.61	25.34	80.59	26.99	75.05	22.25	72.86	22.70
20	67.49	19.72	73.81	23.23	79.81	26.56	75.16	23.98	72.89	22.72
21	66.37	19.09	72.04	22.24	78.66	25.92	75.08	23.93	72.88	22.71
22	65.10	18.39	70.65	21.47	77.51	25.28	74.86	23.81	72.81	22.67
23	57.96	14.42	66.23	19.02	76.44	24.69	74.58	23.66	72.77	22.65
24	55.34	12.97	63.46	17.48	75.24	24.02	74.25	23.47	72.69	22.61

TABLE 16 - MEASURED TEMPERATURES OF WALL C2 FOR NBS-10 TEST CYCLE

Time, hr	Outdoor Chamber Air Temperature, t_o		Outdoor Surface Temperature of Wall, t_2		Internal Wall Temperature, t_3		Indoor Surface Temperature of Wall, t_1		Indoor Chamber Air Temperature, t_i	
	°F	°C	°F	°C	°F	°C	°F	°C	°F	°C
1	34.98	1.66	46.60	8.11	65.65	18.69	71.41	21.89	72.10	22.28
2	33.04	0.58	44.60	7.00	64.30	17.94	71.02	21.68	71.99	22.22
3	32.24	0.13	43.36	6.31	63.06	17.26	70.64	21.47	71.96	22.20
4	32.06	0.03	42.62	5.90	61.85	16.58	70.23	21.24	71.87	22.15
5	33.41	0.78	42.74	5.97	60.80	16.00	69.87	21.04	71.80	22.11
6	44.65	7.03	48.23	9.02	59.93	15.52	69.54	20.86	71.76	22.09
7	56.26	13.48	55.38	12.99	59.60	15.33	69.23	20.68	71.71	22.06
8	64.40	18.00	61.11	16.17	59.93	15.52	69.06	20.59	71.68	22.04
9	70.55	21.42	65.83	18.79	60.73	15.96	68.99	20.55	71.65	22.03
10	76.84	24.91	70.65	21.47	62.06	16.70	69.16	20.64	71.70	22.06
11	80.20	26.78	73.91	23.28	63.45	17.50	69.40	20.78	71.74	22.08
12	83.42	28.57	76.67	24.82	64.95	18.31	69.74	20.97	71.80	22.11
13	89.90	32.17	81.23	27.35	66.46	19.14	70.14	21.19	71.89	22.16
14	92.57	33.65	84.25	29.03	68.12	20.07	70.58	21.43	71.99	22.22
15	89.42	31.90	83.74	28.74	69.79	20.99	71.07	21.71	72.08	22.27
16	84.98	29.43	81.74	27.63	71.21	21.78	71.54	21.97	72.13	22.29
17	77.09	25.05	77.64	25.36	72.25	22.36	71.98	22.21	72.25	22.36
18	63.78	17.66	69.90	21.06	72.70	22.61	72.38	22.43	72.32	22.40
19	54.71	12.62	63.39	17.44	72.52	22.51	72.63	22.57	72.38	22.43
20	49.58	9.77	59.12	15.07	71.69	22.05	72.70	22.61	72.35	22.42
21	48.09	8.93	57.09	13.94	70.57	21.43	72.61	22.56	72.34	22.41
22	47.18	8.43	55.83	13.24	69.37	20.76	72.38	22.43	72.31	22.39
23	40.26	4.59	51.68	10.93	68.21	20.12	72.07	22.26	72.23	22.35
24	37.22	2.90	48.71	9.28	66.97	19.43	71.76	22.09	72.17	22.32

TABLE 17 - RATE OF HEAT FLOW THROUGH WALL C2

Time, hr	Rate of Heat Flow Through Wall, W·hr/hr					
	NBS		NBS+10		NBS-10	
	Measured Q_w	Steady-State Q_{ss}	Measured Q_w	Steady-State Q_{ss}	Measured Q_w	Steady-State Q_{ss}
1	11	-226	91	-156	-59	-306
2	-11	-244	69	-174	-83	-326
3	-38	-255	36	-184	-105	-336
4	-58	-260	22	-185	-130	-340
5	-80	-261	-4	-178	-153	-334
6	-115	-209	-37	-110	-181	-262
7	-128	-117	-51	-17	-201	-171
8	-151	-45	-68	+52	-217	-98
9	-155	18	-78	108	-223	-39
10	-151	77	-70	165	-216	19
11	-143	123	-58	205	-202	56
12	-128	155	-40	238	-183	86
13	-97	202	-16	287	-160	138
14	-76	243	13	319	-134	170
15	-49	238	36	308	-109	157
16	-9	208	70	275	-68	127
17	21	151	106	219	-39	70
18	49	58	131	118	-14	-31
19	71	-29	149	32	3	-115
20	72	-86	160	-17	12	-168
21	77	-114	154	-38	7	-192
22	66	-125	144	-52	-2	-205
23	53	-168	131	-103	-16	-252
24	29	-210	103	-133	-37	-284
Mean	-39	-37	41	41	-105	-110

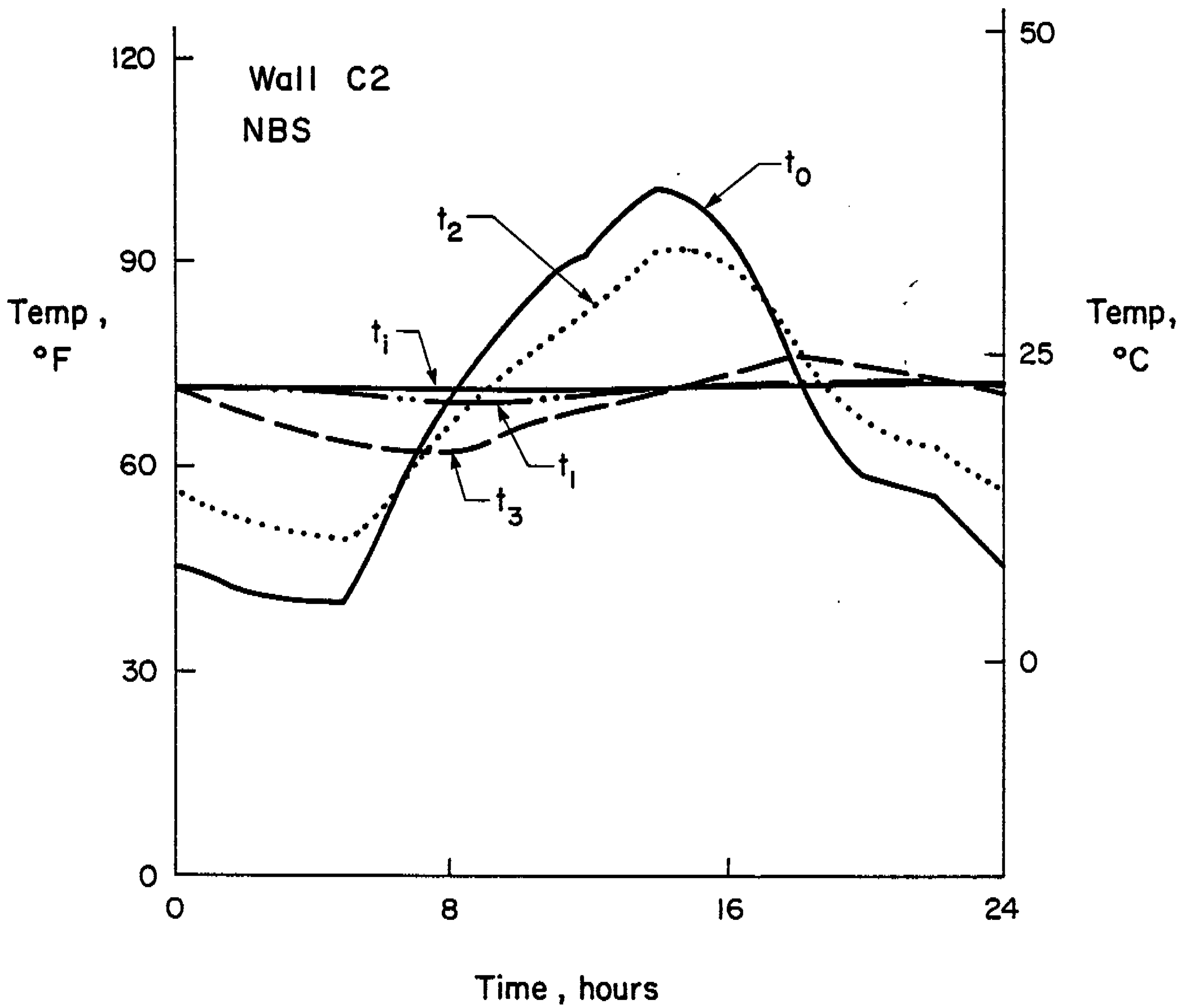

Fig. 21 Measured Temperatures of Wall C2 for NBS Test Cycle

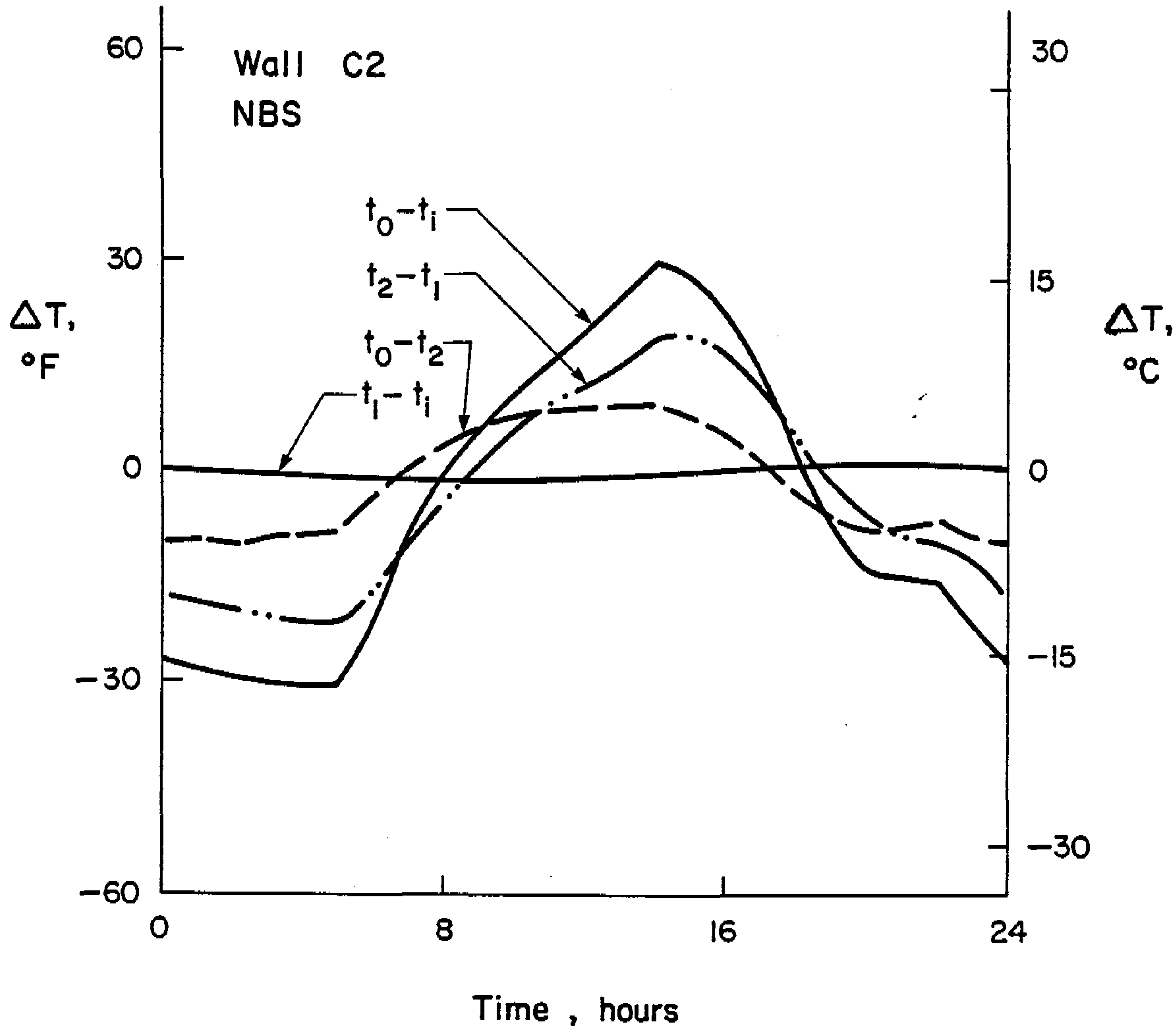

Fig. 22 Measured Temperature Differentials of Wall C2 for NBS Test Cycle

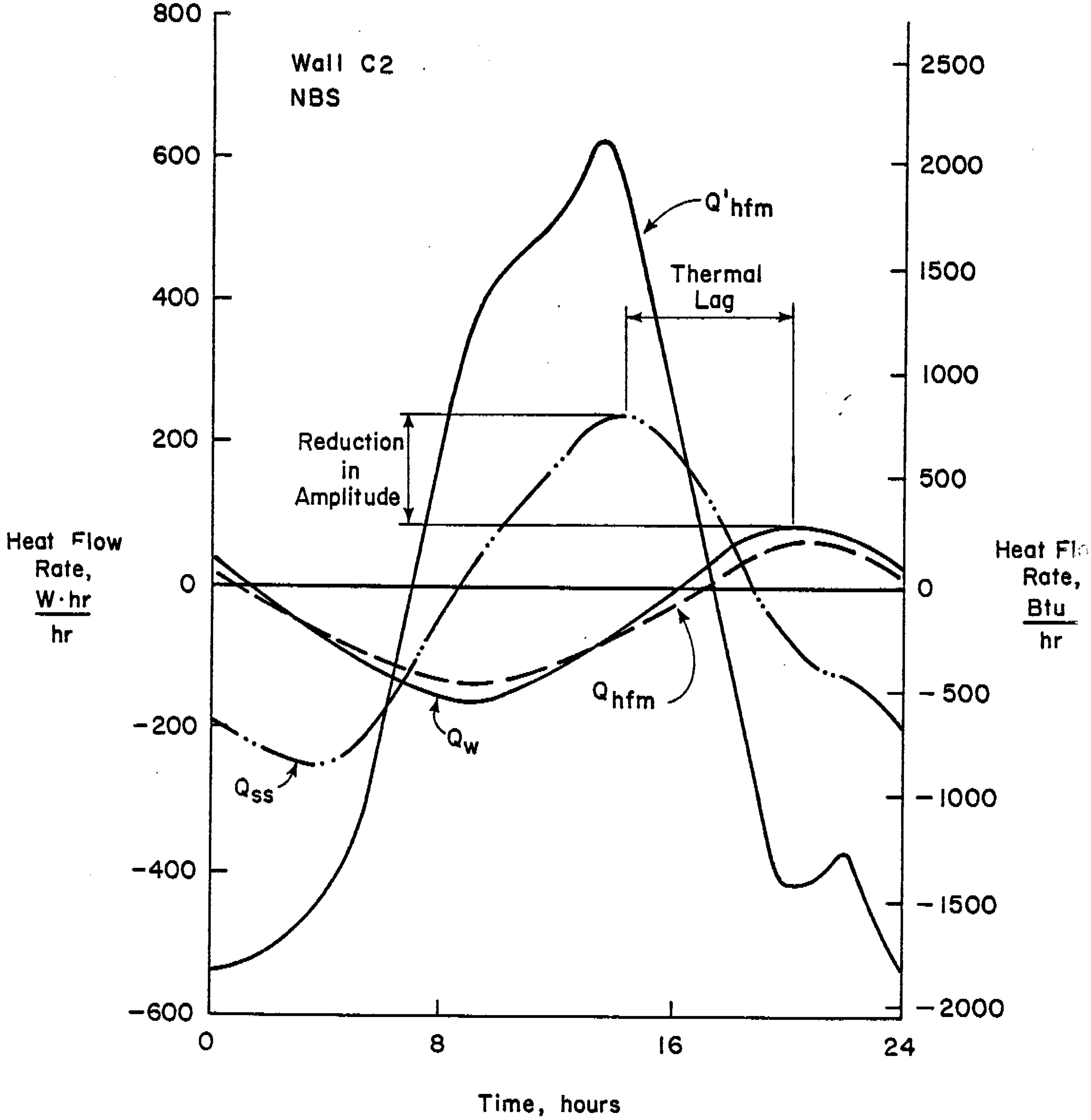

Fig. 23 Rate of Heat Flow Through Wall C2 for NBS Test Cycle

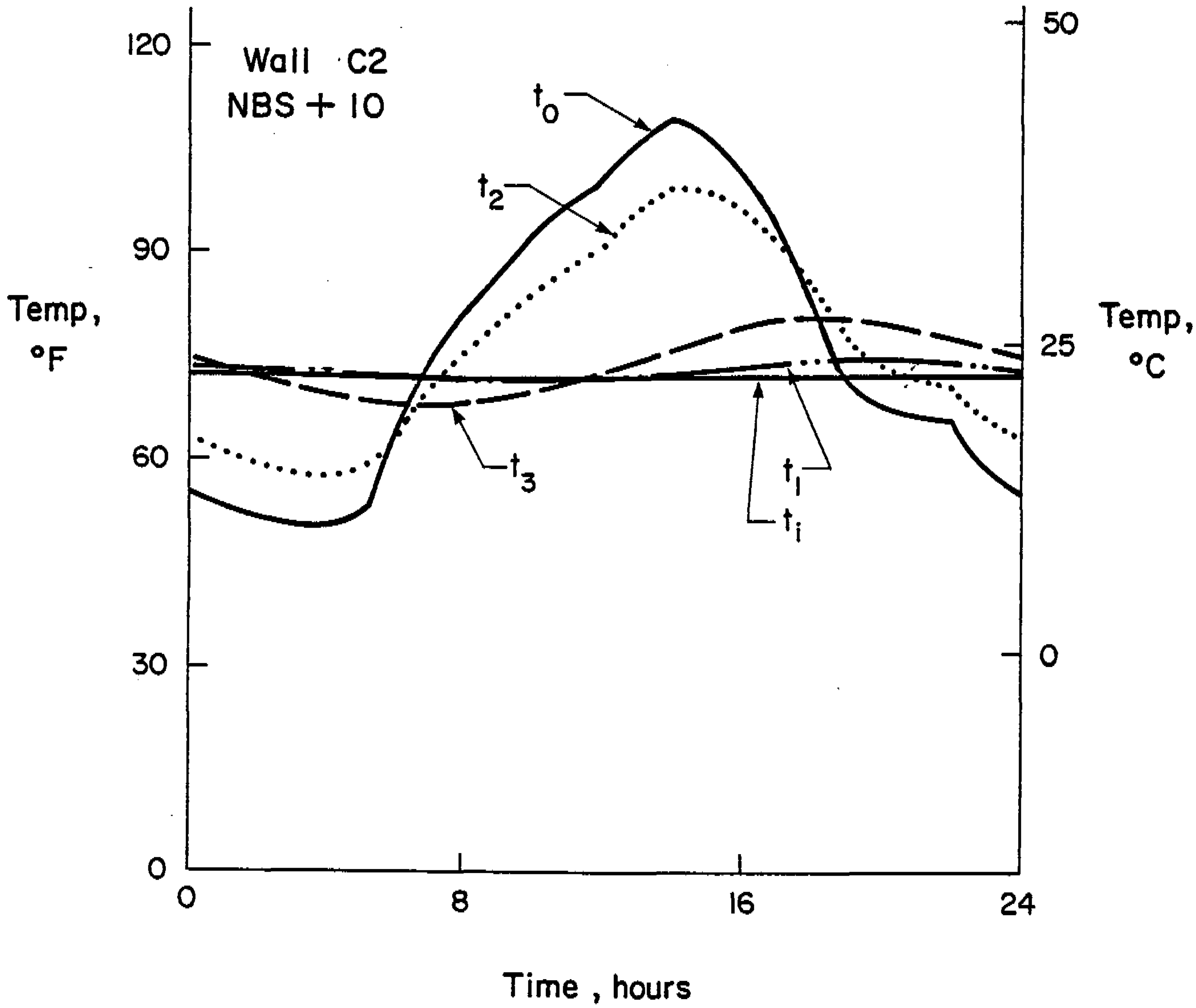

Fig. 24 Measured Temperatures of Wall C2 for NBS+10 Test Cycle

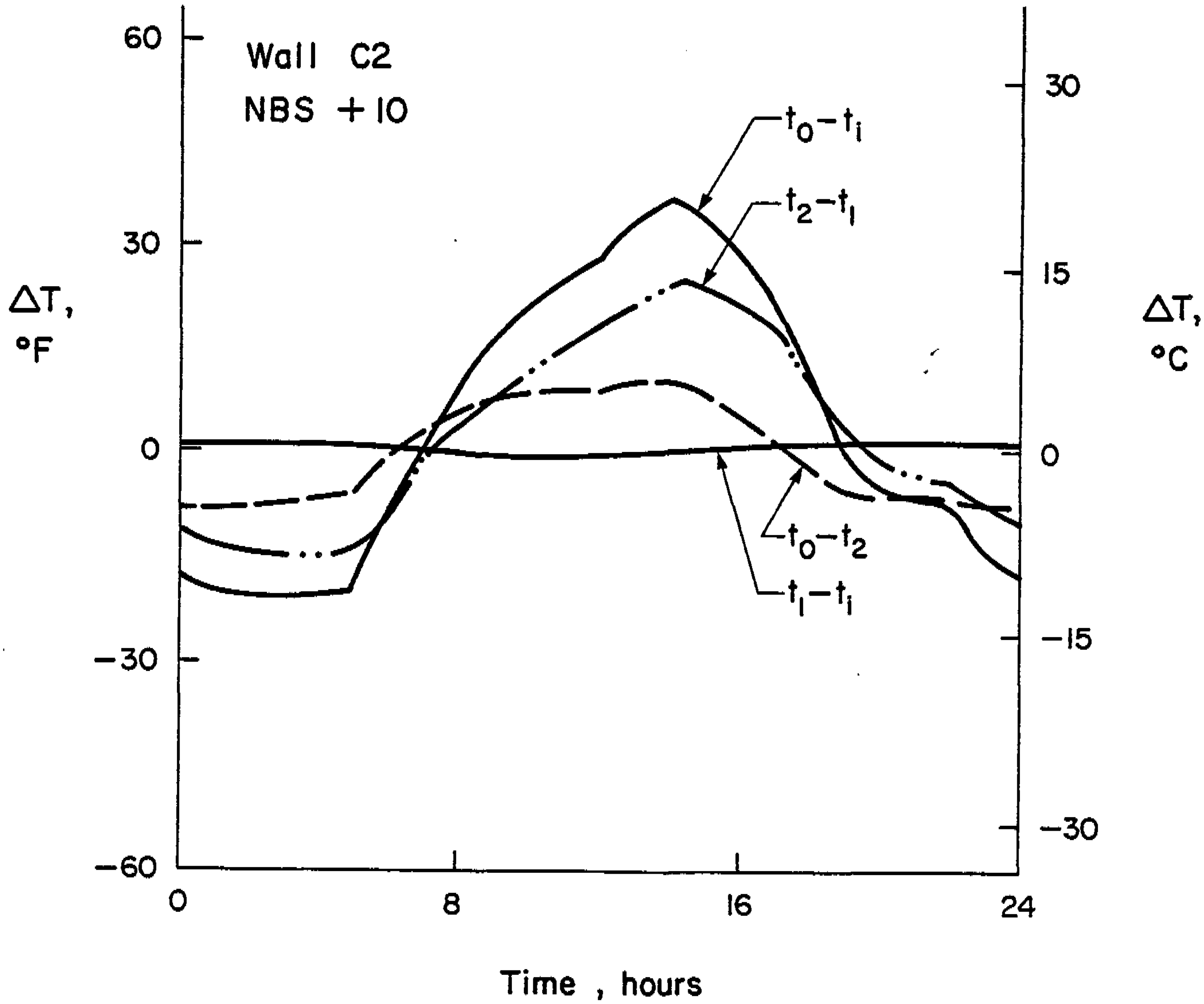

Fig. 25 Measured Temperature Differentials of Wall C2 for NBS+10 Test Cycle

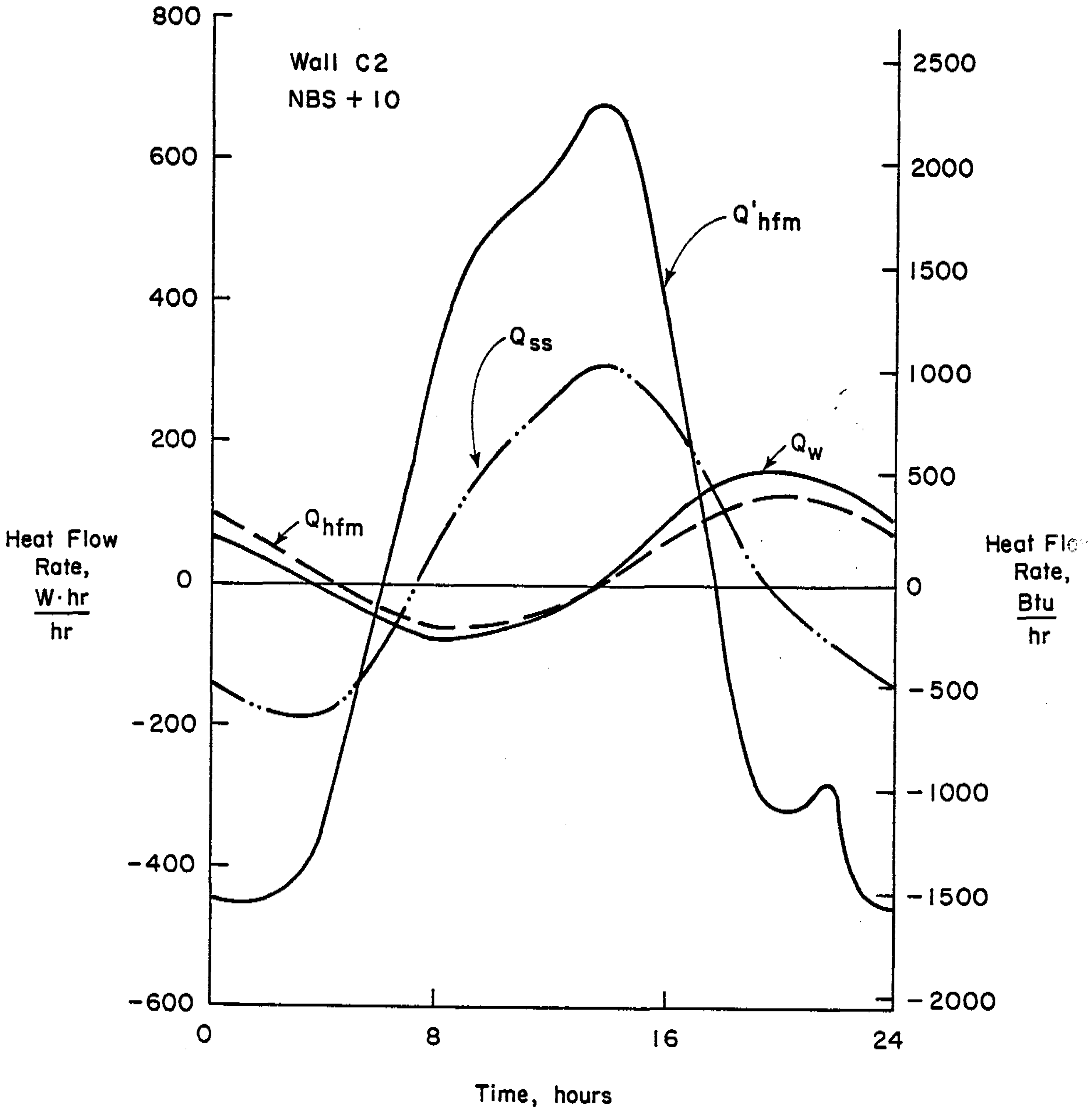

Fig. 26 Rate of Heat Flow Through Wall C2 for NBS+10 Test Cycle

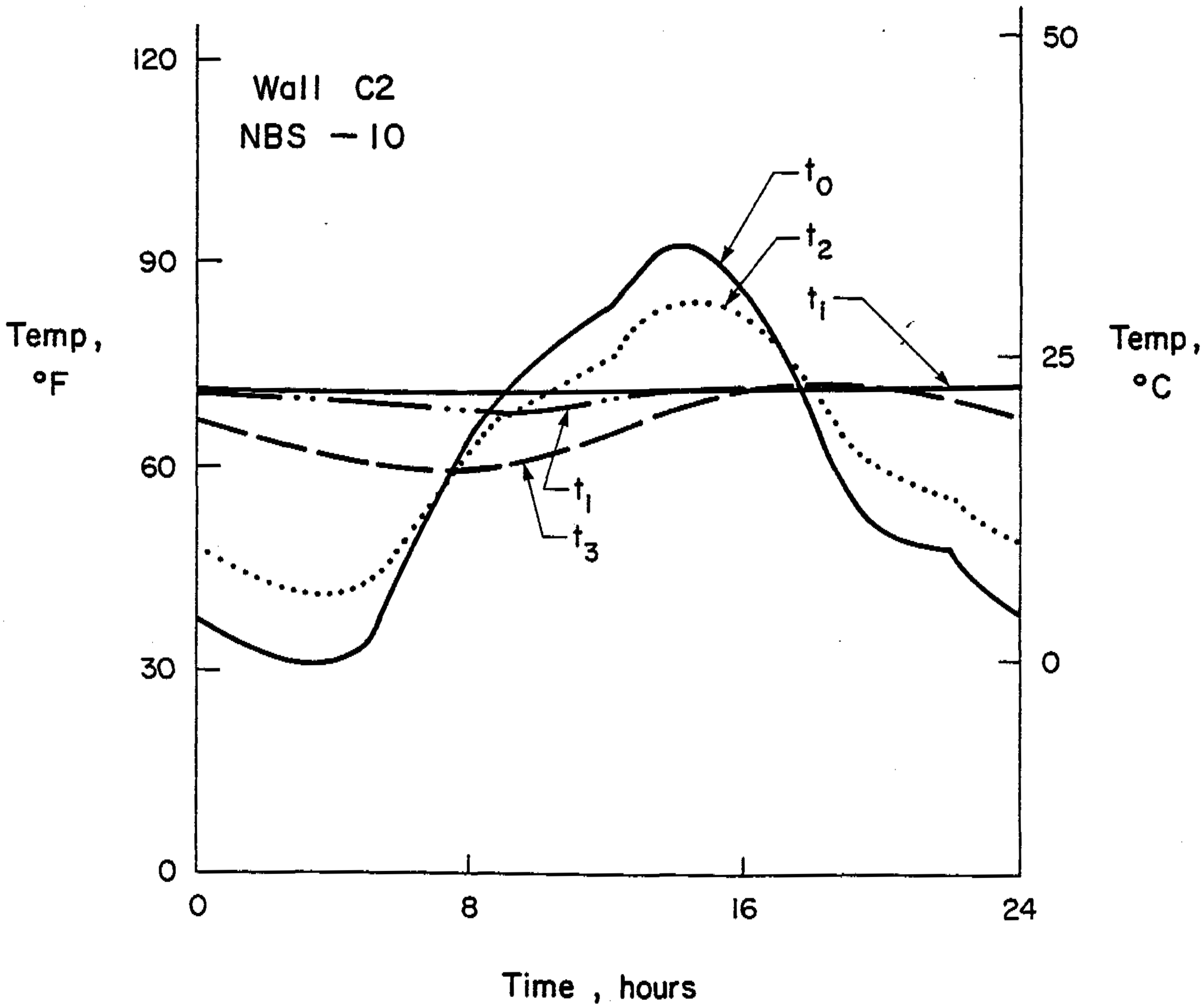

Fig. 27 Measured Temperatures of Wall C2 for NBS-10 Test Cycle

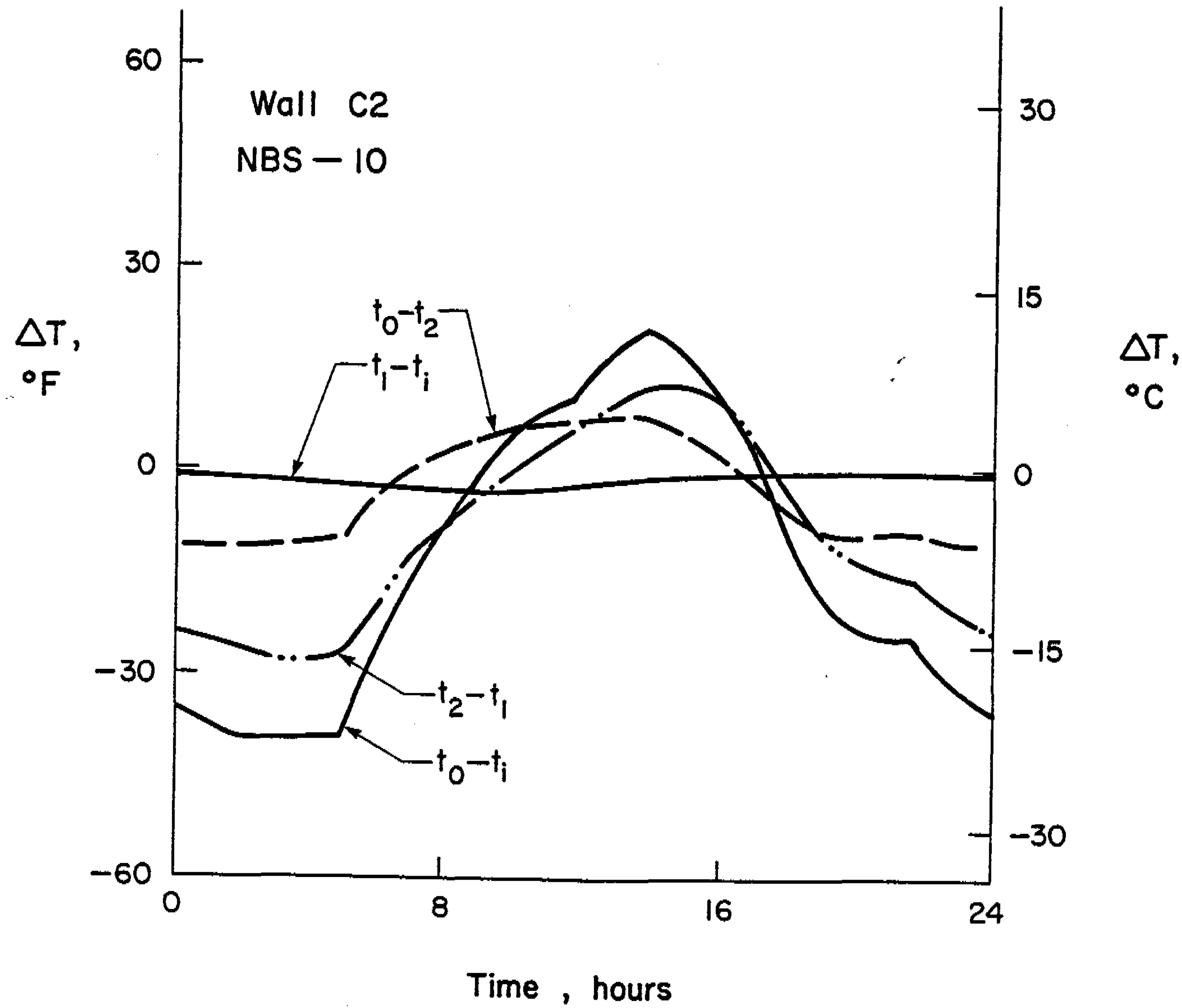

Fig. 28 Measured Temperature Differentials of Wall C2 for NBS-10 Test Cycle

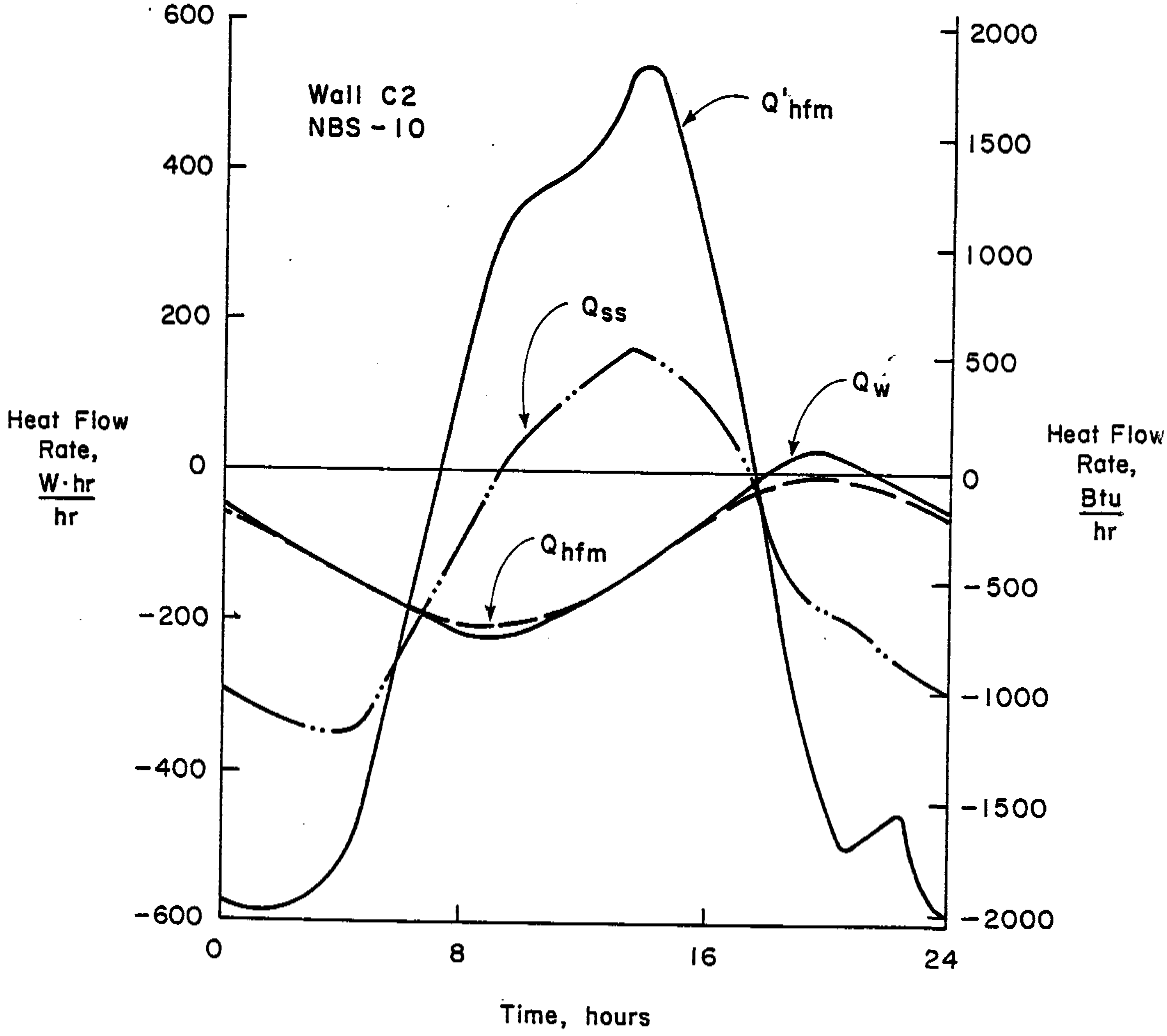

Fig. 29 Rate of Heat Flow Through Wall C2 for NBS-10 Test Cycle

wall temperatures. Air-to-air, surface-to-surface, and surface-to-air temperature differentials are illustrated in Figs. 22, 25, and 28. Notation used to designate average measured temperatures is repeated here for convenience:

t_i = indoor chamber air temperature

t_1 = wall surface temperature, indoor side

t_3 = internal wall temperature at approximate midthickness

t_2 = wall surface temperature, outdoor side

t_o = outdoor chamber air temperature

Table 17 and Figs. 23, 26, and 29 present Q_w, measured heat flow rates through Wall C2, calculated from Eq. (1). Heat flow rates measured by heat flow meters mounted on the indoor surface of Wall C2, Q_{hfm}, and on the outdoor wall surface, Q'_{hfm}, are also shown. Heat flow rates predicted by steady-state analysis are shown by the curve designated Q_{ss}. Positive values represent heat flow from the outdoor to the indoor side of the wall. All data represent averages from three consecutive 24-hour cycles.

Heat flow meter data were calibrated using results of steady-state calibrated hot box tests of Wall C2. Heat flow meter readings were plotted against measured heat flow rates, Q_w, for the four steady-state tests. The slope of the line through the four points was used as a calibration factor.

Heat flow rates predicted by steady-state analysis were calculated on an hourly basis from wall surface temperatures using Eq. (3). Peaks in the Q_{ss} curve occur where differences in temperature between the outdoor and indoor wall surfaces are the greatest.

Peaks in the measured heat flow curve, Q_w, have smaller amplitudes and occur at a later time than those on the Q_{ss} curve. The reduction in amplitude and thermal lag are due to the storage capacity of lightweight concrete.

Thermal Lag

Thermal lag is a measure of the response of both inside and outside surface temperatures and heat flow to fluctuations in outdoor temperature. Lag is indicative of both thermal resistance and heat storage capacity of the test specimen, since both of these factors influence the rate of heat flow.

Thermal lag is quantified by two measures in Table 18. In one measure, lag was calculated as the time required for the maximum or minimum indoor surface temperature to be reached after the maximum or minimum outdoor air temperature was attained. In the second measure, lag was calculated as the time required for the maximum or minimum heat flow rate, Q_w, to be reached after the maximum or minimum heat flow rate based on steady-state predictions, Q_{ss}, was attained. This is illustrated in Fig. 23. As can be seen from Table 18, both measures gave similar results. Results were also similar for each of the test cycles. Average lag for the NBS and NBS-10 cycles was 5.5 hours. The NBS+10 cycle had an average lag of 6 hours.

TABLE 18 - SUMMARY OF DYNAMIC TEST RESULTS FOR WALL C2

Test Cycle	Thermal Lag, hrs					Reduction in Amplitude, percent			Total Energy, W·hr			Net Energy, W·hr		
	t_o vs t_1		Q_{ss} vs Q_w		Avg.									
	@ Max	@ Min	@ Max	@ Min		@ Max	@ Min	Avg.	Q'_a	Q'_b	Q'_a/Q'_b	Measured	Calculated	Meas./Calc.
NBS	6	5	7	4.5	5.5	59	48	54	1838	3822	0.48	-940	-876	1.07
NBS+10	6	6	6	5.5	6	57	47	52	1837	3673	0.50	993	979	1.01
NBS-10	6	5	6	5	5.5	57	50	54	2554	4282	0.60	-2510	-2636	0.95

Data from the heat flow meter mounted on the indoor surface of Wall C2, denoted Q_{hfm} in the figures, consistently show the same lag time as measured heat flow, Q_w.

Thermal lag is of interest because the time of occurrence of peak heat flows will have an effect on overall response of the building envelope. If the envelope can be effectively used to delay the occurrence of peak loads, it may be possible to improve overall energy efficiency. The "lag effect" is also of interest for passive solar applications.

Reduction in Amplitude

The reduction in amplitude, or damping, is influenced by the same factors as thermal lag. Both thermal resistance and heat storage capacity affect damping. The damping effect can be seen in Fig. 23.

Values for percent reduction in amplitude listed in Table 18 were calculated using the following equation:

$$A = [1 - (Q'_w - \bar{Q}_w)/(Q'_{ss} - \bar{Q}_w)]\cdot 100 \qquad (11)$$

where:

A = percent reduction in amplitude

$\bar{Q}_w$ = mean measured heat flow through wall

Q'_w = maximum or minimum measured heat flow through wall

Q'_{ss} = maximum or minimum heat flow through wall predicted by steady-state analysis

As shown in Table 18, average reduction in amplitude for the three cycles was between 52 and 54%.

Actual maximum heat flow through a wall is important in determining the peak energy load for a building envelope. If peak heat flows are reduced, peak energy demands will decrease. Storage capacity as well as thermal transmittance of each wall in a building envelope influence peak energy requirements.

Amplitudes for indoor surface heat flow meter data, Q_{hfm}, are less than amplitudes for measured heat flow, Q_w. This occurs for all dynamic cycles and is illustrated in Figs. 23, 26, and 29. Amplitudes for Q_{hfm} and Q_w differ because of the physical effect of a heat flow meter mounted on a wall. Heat flow paths are altered at the location of the heat flow meter. Heat flow meter calibration using steady-state results does not correct for dynamic effects of the meter location.

Measured Energy

Results of dynamic tests were also compared using measures of energy expended in maintaining constant indoor temperature while outdoor temperatures were varied. Energy expended is a measure of heat flow through the test wall. It should be noted that comparison of measured energy values for the test walls is limited to specimens and dynamic cycles evaluated in this program. Results are for diurnal test cycles and should not be arbitrarily assumed to represent annual heating and cooling loads. In addition, results are for individual opaque wall assemblies. As such, they are representative of only one component of the building envelope.

Two parameters were derived as measures of energy expended, or heat flow through the test walls, during dynamic cycles. These are illustrated in Fig. 30. The curve marked "Q_w" is a

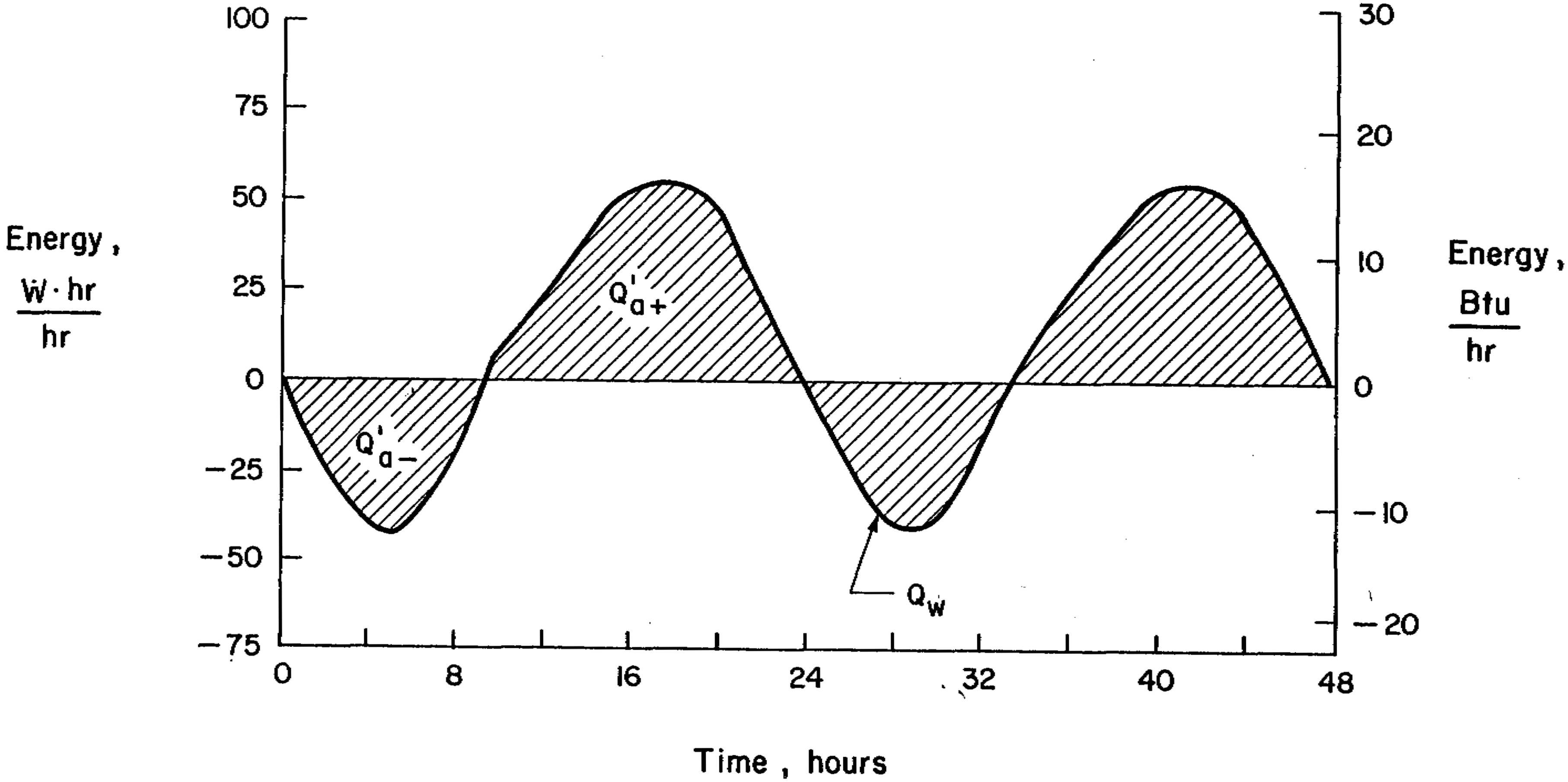

Fig. 30 Definition of Measured Energy

measure of heat flow through the test wall. Results were corrected for heat extracted by indoor cooling and for heat transfer to laboratory space using Eq. (1), as previously described.

Areas within "loops" of the measured energy curves were used to provide an indication of total energy expended. These areas are denoted as Q'_{a+} and Q'_{a-} in Fig. 30. The sum of the absolute values of positive and negative areas is taken to represent total energy over a 24-hr period. This value is denoted as Q'_a in Table 18.

A similar procedure is used to calculate total energy based on steady-state predictions over a 24-hr period. This value, denoted Q'_b in Table 18, is the sum of the absolute values of positive and negative areas under a steady-state curve.

Values of Q'_a, Q'_b, and Q'_a/Q'_b for each test cycle are listed in Table 18. For all three test cycles, total measured energy, Q'_a, was considerably less than total energy based on steady-state predictions, Q'_b.

Measured net energy theoretically should be equal to net energy based on steady-state predictions. Measured net energy for a 24-hr periodic cycle is equal to the sum of hourly measured rates of heat flow. These values can be found by totalling values of "Q_w" in columns of Table 17. Steady-state net energy was calculated according to the following equation:

$$Q_n = \frac{C \cdot A \cdot (t_1^m - t_2^m) \cdot 24}{3.413} \tag{12}$$

where:

Q_n = net energy based on steady-state predictions

A = area of wall surface normal to heat flow, ft^2

t_1^m = mean temperature of inside wall surface over 24-hr cycle, °F

t_2^m = mean temperature of outside wall surface over 24-hr cycle, °F

3.413 = conversion factor from W·hr/hr to Btu/hr

C = average measured thermal conductance, $Btu/hr \cdot ft^2 \cdot °F$

The value Q_n can also be found by summing values of "Q_{ss}" in columns of Table 17.

A comparison of calculated and measured net energy data is given in Table 18. Measured and calculated values agree to within 7%, which indicates that measured data are reasonable.

Cycles with net heat flow close to zero have greater total energy savings. For example, Q_a'/Q_b' is least for the NBS cycle. This is also the cycle with net heat flow through Wall C2 closest to zero.

THERMAL PROPERTIES OF CONCRETE UNDER TRANSIENT TEST CONDITIONS

Time required for a wall to reach a steady-state condition can be determined from transient tests. This time is affected by both thermal resistance and heat storage capacity of the test wall.

Test Procedure

Results of a transient test are determined from data collected in the period of time between two steady-state tests.

After a wall is in a steady-state condition, the outdoor chamber temperature setting is changed. The transient test continues until the wall reaches an equilibrium for the new outdoor chamber air temperature.

For Wall C2, energy required to maintain a constant indoor temperature was monitored as a function of time. The rate of heat flow through Wall C2 was determined using Eq. (1) for hourly averages of data.

Transient Test Results

Transient test results, illustrated in Figs. 31, 32, and 33, are for initial and final wall mean temperatures of 72.8°F (22.7°C) and 33.9°F (1.0°C), respectively. Figure 31 gives measured air, surface, and internal wall temperatures. Air-to-air, surface-to-surface, and surface-to-air temperature differentials are illustrated in Fig. 32.

Figure 33 presents Q_w, measured heat flow, and Q_{ss}, heat flow predicted by steady-state analysis. Heat flow rates measured by a heat flow meter mounted on the indoor surface of Wall C2, Q_{hfm}, and on the outdoor wall surface, Q'_{hfm}, are also shown. Values of Q_{ss} were calculated on an hourly basis from wall surface temperatures using Eq. (3). Heat flow meter data were calibrated using results of steady-state calibrated hot box tests. The values of Q_{ss} and Q_w are equivalent after 43 hours of testing. However, Q_{ss} approached the final heat flow rate more rapidly than Q_w.

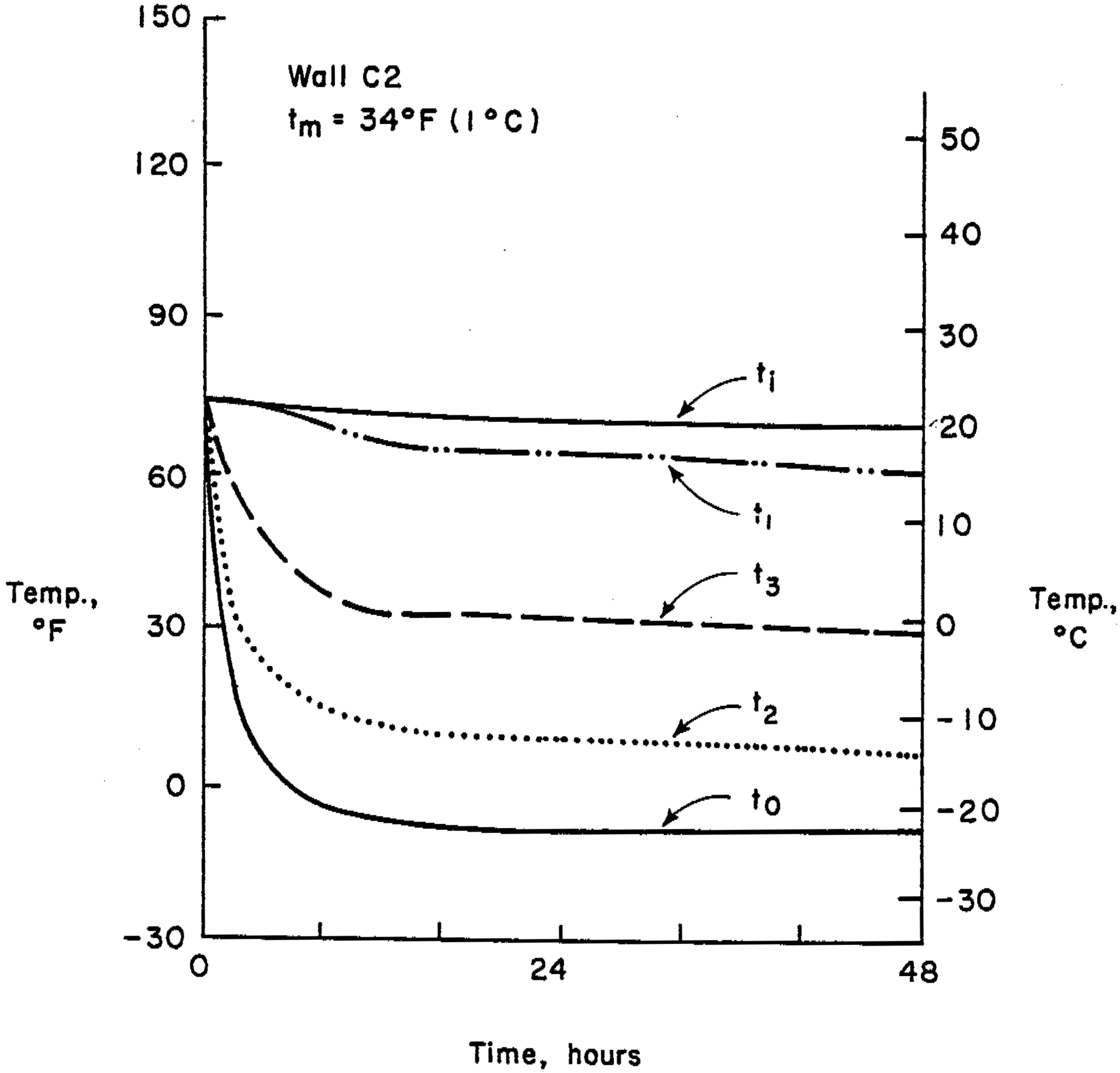

Fig. 31 Measured Temperatures of Wall C2 for Transient Test

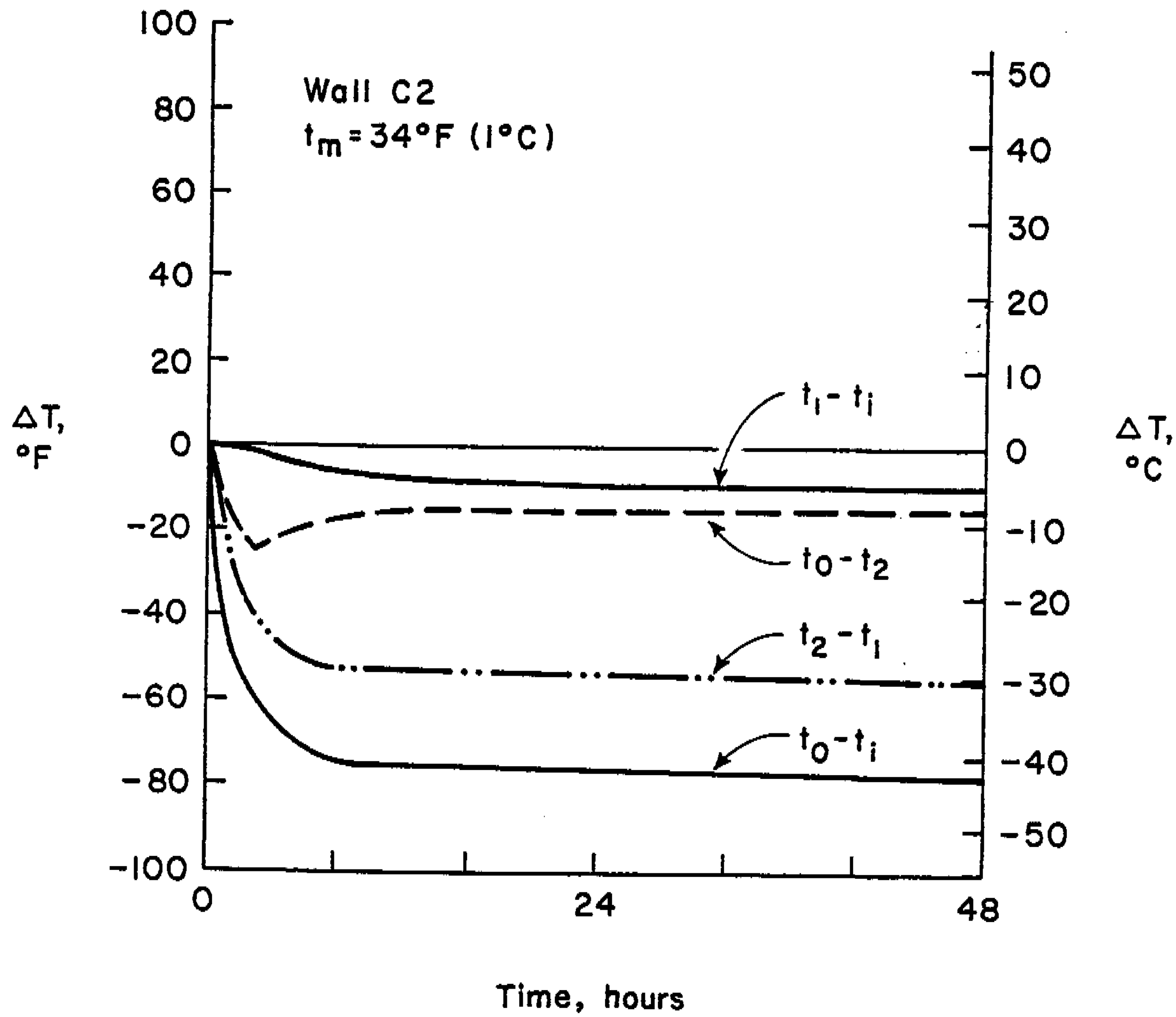

Fig. 32 Measured Temperature Differentials of Wall C2 for Transient Test

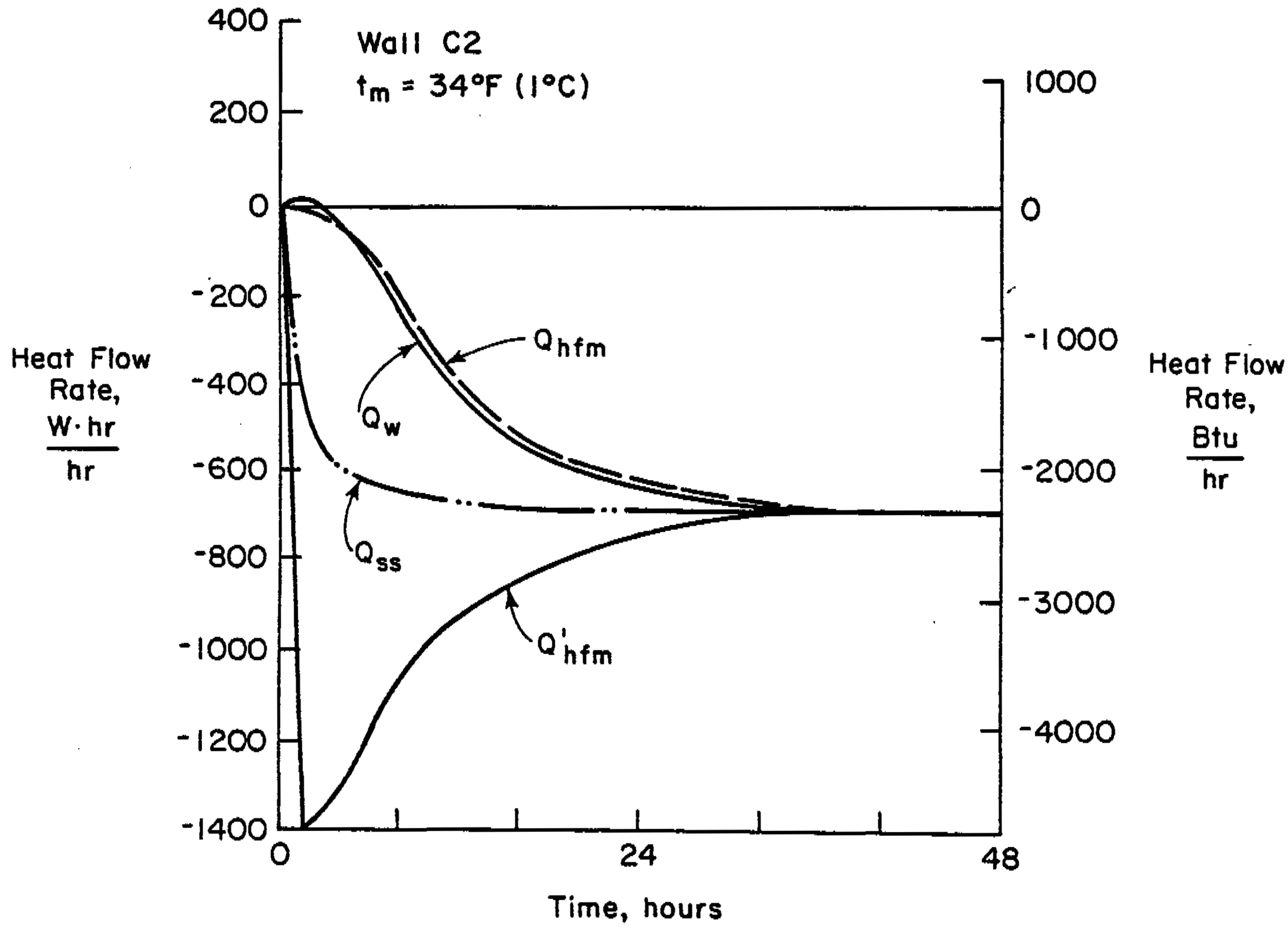

Fig. 33 Rate of Heat Flow Through Wall C2 for Transient Test

Results of this transient test are summarized in Table 19. Calibrated hot box test results show that Wall C2 reached 95% of the final heat flow rate after 29 hours. Heat flow rates based on steady-state analysis predicted 95% of the final heat flow rate would be reached after 9 hours. Similarly, 90% of the final heat flow rate was measured as occurring after 24 hours, and was predicted to occur after 6 hours. The amount of time required for Wall C2 to reach 90% of the final heat flow rate was four times greater than steady-state predictions.

This delayed response time of Wall C2 when compared to predicted response based on steady-state analysis is similar to the effect of thermal lag. Transient test results show that Wall C2 prolonged the consequences of a sudden change in outdoor chamber air temperature. If the building envelope can be effectively used to delay the occurrence of peak loads, it may be possible to improve overall energy efficiency.

SUMMARY AND CONCLUSIONS

This report presents results of an experimental investigation of heat transmission characteristics for a structural lightweight concrete wall under steady-state and dynamic temperature conditions. Companion structural lightweight concrete control specimens were also tested to determine physical and thermal properties.

The following conclusions are based on results obtained in this investigation.

TABLE 19 - SUMMARY OF TRANSIENT TEST RESULTS FOR WALL C2

	Measured Q_w, W•hr/hr	Time Required to reach Q_w, hr	Steady-State Q_{ss}, W•hr/hr	Time Required to reach Q_{ss}, hr
Final Heat Flow Rate	- 672	43	- 672	22
95% of Final Heat Flow Rate	- 638	29	- 638	9
90% of Final Heat Flow Rate	- 605	24	- 605	6

1. Specific heat of Wall C2 was 0.230 Btu/lb·°F (960 J/kg·°K) at a moisture content of 8.5% relative to ovendry weight.
2. Apparent thermal conductivity of Wall C2 derived from steady-state calibrated hot box tests was 4.7 Btu·in./hr·ft^2·°F (0.68 W/m·°K).
3. Apparent thermal conductivity of ovendry concrete found using ASTM Designation: C177 with embedded thermocouples was 4.5 Btu·in./hr·ft^2·°F (0.65 W/m·°K).
4. Measured conductivity of air dry concrete determined from the hot wire method was 6.0 Btu·in./hr·ft^2·°F (0.87 W/m·°K).
5. Measured thermal diffusivity of a saturated specimen with the same mix design as Wall C2 was 0.0155 ft^2/hr (0.400 mm^2/s).
6. Measured total thermal resistance (R_T) and thermal transmittance (U) for Wall C2 were 2.6 hr·ft^2·°F/Btu (0.46 m^2·°K/W) and 0.39 Btu/hr·ft^2·°F (2.2 W/m^2·°K), respectively.
7. As indicated by thermal lag, heat storage capacity of Wall C2 delayed heat flow through the specimen. Average thermal lags for the three test cycles ranged from 5.5 to 6.0 hours.
8. As indicated by the damping effect, heat storage capacity of Wall C2 reduced peak heat flows through the specimen. Average reductions in amplitude of Wall C2 for the three test cycles ranged from 52 to 54%.

9. For the three diurnal temperature cycles, energy requirements for a 24-hour period varied considerably. Cycles with net heat flow closer to zero had greater total energy savings. Total measured heat flows over the 24-hour cycles tested ranged from 48 to 60% of those predicted by steady-state analysis. These reductions in total heat flow are attributed to effects of thermal mass.

10. Transient test results indicate that heat storage capacity of Wall C2 delayed heat flow through the specimen. The amount of time required for the specimen to reach a steady-state condition was also delayed.

Results described in this report provide data on thermal response of a structural lightweight concrete wall subjected to steady-state and diurnal sol-air temperature cycles. A complete analysis of building energy requirements must include consideration of the entire building envelope, the building orientation and operation, and yearly weather conditions. Data developed in this experimental program provide a quantitative basis for modeling the building envelope, which is part of the overall energy analysis process.

ACKNOWLEDGMENTS

This paper was prepared as part of a project sponsored jointly by the U.S. Department of Energy, Office of Buildings Energy Research and Development, and the Portland Cement Association. The work is under subcontract ORNL/SUB-42539/1 with Oak Ridge National Laboratory (ORNL). It is part of the National Program Plan for Building Thermal Envelope Systems and Insulating Materials.

The work was performed in the Engineering Development Division of the Construction Technology Laboratories (CTL), a Division of the Portland Cement Association, under the direction of Dr. W. G. Corley, Divisional Director.

Construction of the structural lightweight concrete wall was sponsored by the Solite Corporation, West New York, N. J. In addition, expanded shale aggregate used in the mix was provided by the Solite Corporation.

Exterior coating materials for Wall C2 were provided by Thoro System Products. Advice and assistance on application of the coatings were provided by Mr. W. Downs and Mr. S. Downs of Thoro System Products, Buffalo Grove, Illinois.

Construction and preparation of specimens were performed by Mr. L. S. Johal, Mr. E. A. Valko, Mr. J. A. Chavez, and Mr. P. P. Hordorwich. Mr. J. A. Chavez also assisted with data reduction. Mr. J. T. Julien monitored Wall C2 calibrated hot box tests.

Mr. D. W. Musser, Director, Construction Methods Department reviewed the manuscript and provided helpful comments and suggestions.

Mrs. E. Ringquist provided editorial assistance in preparation of the manuscript. The manuscript was typed by personnel of the Portland Cement Association's Word Processing Department. Mr. R. Kuhart and Mr. R. Reichenbach drafted the figures.

REFERENCES

1. Fiorato, A. E. and Bravinsky, E., "Heat Transfer Characteristics of Walls Under Arizona Temperature Conditions," Construction Technology Laboratories, Portland Cement Association, Skokie, 1981, 61 pp.

2. Fiorato, A. E. and Cruz, C. R., "Thermal Performance of Masonry Walls," Research and Development Bulletin RD071, Portland Cement Association, Skokie, 1980, 17 pages.

3. Fiorato, A. E., "Heat Transfer Characteristics of Walls Under Dynamic Temperature Conditions," Research and Development Bulletin RD075, Portland Cement Association, Skokie, 1981, 20 pages.

4. Van Geem, M. G., Fiorato, A. E., and Julien, J. T., "Heat Transfer Characteristics of a Normal-Weight Concrete Wall," Construction Technology Laboratories, Portland Cement Association, Skokie, 1983, 89 pp.

5. Van Geem, M. G. and Fiorato, A. E., "Heat Transfer Characteristics of a Low Density Concrete Wall," to be published, Construction Technology Laboratories, Portland Cement Association, Skokie.

6. <u>Design and Control of Concrete Mixtures</u>, PCA Bulletin EB001.12T, Portland Cement Association, Skokie, 1979, p. 36.

7. Brewer, Harold W., "General Relation of Heat Flow Factors to the Unit Weight of Concrete," <u>Journal of the PCA Research and Development Laboratories</u>, Vol. 9, No. 1, January 1967, pages 48-60.

8. 1983 Annual Book of ASTM Standards, American Society for Testing and Materials, Philadelphia, to be published.

9. Fiorato, A. E., "Laboratory Tests of Thermal Performance of Exterior Walls," Proceedings of the ASHRAE/DOE-ORNL Conference on Thermal Performance of the Exterior Envelopes of Buildings, Orlando, Florida, Dec. 1979, ASHRAE SP28, New York, 1981, pp. 221-236.

10. Van Geem, M. G., Fiorato, A. E., and Musser, D. W., "Calibration and Test Procedures for the Calibrated Hot Box Method of Evaluating Thermal Performance," to be published, Construction Technology Laboratories, Portland Cement Association, Skokie.

11. ASHRAE Handbook of Fundamentals, American Society of Heating, Refrigeration, and Air-Conditioning Engineers, Inc., New York, 1981.

12. "Method of Test for Specific Heat of Aggregates, Concrete, and Other Materials (Method of Mixtures)," Handbook for Concrete and Cement, U.S. Army Waterways Experimental Station, Vicksburg, CRD-C124-73, 3 pages.

13. Whiting, D., Litvin, A., and Goodwin, S. E., "Specific Heat of Selected Concretes," Journal of the American Concrete Institute, July 1978, pages 299-305. Also PCA Research and Development Bulletin RD058.

14. Desjarlais, Andre, "The Thermal Conductivity and Thermal Resistance of Three Specimens of Concrete Materials," Dynatech Report No. PCA-1, Dynatech R/D Company, Cambridge, 4 pages.

15. Tye, R. P., and Spinney, S. C., "Thermal Conductivity of Concrete: Measurement Problems and Effect of Moisture," Presented at Meeting of Commission of BI of Institute International Du Froid, Washington, D. C., September 14-15, 1976, Dynatech R/D Company, Cambridge.

16. Lentz, A. E., and Monfore, G. E., "Thermal Conductivity of Concrete at Very Low Temperatures," Journal of the PCA Research and Development Laboratories, Vol. 7, No. 2, May 1965, pages 39-46.

17. Van Geem, M. G. and Fiorato, A. E., "Thermal Properties of Masonry Materials for Passive Solar Design - A State-of-the-Art Review," Construction Technology Laboratories, Portland Cement Association, Skokie, 86 pages.

18. Valore, Rudolph V. C. Jr., "Calculation of U-Values of Hollow Concrete Masonry," Concrete International, Vol. 2, No. 2, February 1980, pages 40-63.

19. "Method of Test for Thermal Diffusivity of Concrete," Handbook for Concrete and Cement, U.S. Army Waterways Experimental Station, Vicksburg, CRD-C36-73, 3 pages.

20. Billington, N. S., "The Thermal Diffusivity of Some Poor Conductors," Journal of Scientific Instruments, Vol. 26, January 1949, pages 20-33.

21. Peavy, B. A., Powell, F. J., and Burch, D. M. "Dynamic Thermal Performance of an Experimental Masonry Building," Building Science Series 45, U.S. Department of Commerce, National Bureau of Standards, Washington D. C., July 1973.